Heliyon 10 (2024) e37123

Contents lists available at ScienceDirect

Heliyon

journal homepage: www.cell.com/heliyon

Review article

Exploring nanomaterial-modified biochar for environmental remediation applications

Neda Arabzadeh Nosratabad [a,1], Qiangu Yan [b,1], Zhiyong Cai [b,**], Caixia Wan [a,*]

[a] Department of Chemical and Biomedical Engineering, University of Missouri, 1406 East Rollins Street, Columbia, MO, 65211, USA
[b] Forest Products Laboratory, USDA Forest Service, One Gifford Pinchot Drive, Madison, WI, 53726-2398, USA

ARTICLE INFO

Keywords:
Nanomaterial-modified biochar
Biomass
Metal nanoparticles
Environmental remediation
Nanotechnology

ABSTRACT

Environmental pollution, particularly from heavy metals and toxic elements, poses a significant threat to both human health and ecological systems. While various remediation technologies exist, there is an urgent need for cost-effective and sustainable solutions. Biochar, a carbon-rich product derived from the pyrolysis of organic matter, has emerged as a promising material for environmental remediation. However, its pristine form has limitations, such as low adsorption capacities, a relatively narrow range of pH adaptability which can limit its effectiveness in diverse environmental conditions, and a tendency to lose adsorption capacity rapidly in the presence of competing ions or organic matters. This review aims to explore the burgeoning field of nanomaterial-modified biochar, which seeks to overcome the limitations of pristine biochar. By incorporating nanomaterials, the adsorptive and reactive properties of biochar can be significantly enhanced. Such modifications, especially biochar supported with metal nanoparticles (biochar-MNPs), have shown promise in various applications, including the removal of heavy metals, organic contaminants, and other inorganic pollutants from aqueous environments, soil, and air. This review provides a comprehensive overview of the synthesis techniques, characterization methods, and applications of biochar-MNPs, as well as discusses their underlying mechanisms for contaminant removal. It also offers insights into the advantages and challenges of using nanomaterial-modified biochar for environmental remediation and suggests directions for future research.

1. Introduction

In recent years, there have been growing concerns over the escalating contamination of soil, water, and air. One of the most pressing concerns is the contamination of soil and water with heavy metals and toxic elements, such as lead (Pd), arsenic (As), mercury (Hg), and chromium (Cr), in natural ecosystems [1–7]. These elements are not only highly toxic but also resistant to degradation, leading to their accumulation in the environment. The bioaccumulation of these toxicants can have detrimental effects on human health, often through the soil-plant-animal-human biological chain [8]. Air pollution is another critical environmental concern. Driven by industrial activities, vehicle emissions, and agricultural practices, air pollution introduces a variety of harmful substances into the

* Corresponding author.
** Corresponding author.
E-mail addresses: zhiyong.cai@usda.gov (Z. Cai), wanca@missouri.edu (C. Wan).
[1] These authors contributed equally.

https://doi.org/10.1016/j.heliyon.2024.e37123
Received 4 March 2024; Received in revised form 27 August 2024; Accepted 28 August 2024
Available online 29 August 2024
2405-8440/© 2024 The Authors. Published by Elsevier Ltd. This is an open access article under the CC BY-NC license (http://creativecommons.org/licenses/by-nc/4.0/).

atmosphere, including nitrogen oxides (NO_x), sulfur oxides (SO_x), volatile organic compounds (VOCs), and greenhouse gases (GHGs) such as carbon dioxide (CO_2) and methane (CH_4) [9]. These pollutants can cause severe health problems, including respiratory and cardiovascular diseases, and contribute to global climate change [10,11]. The persistence and bioaccumulative nature of these contaminants make it imperative to develop effective and sustainable remediation technologies. For example, remediation of heavy metal-contaminated soil and water has primarily relied on conventional techniques such as chemical precipitation, ion exchange, and membrane filtration [12]. While these methods have shown some efficacy, they come with their own challenges, such as use of additional reagents, high membrane costs, and fouling. Micro/nano plastic pollution further highlight the need for effective remediation strategies to mitigate environmental and health risks [13].

In the context of environmental pollution, biochar has emerged as a promising solution to various environmental challenges [14]. Biochar is rich in carbon, fine-grained, porous, and has large surface areas. It is produced by pyrolyzing biomass materials, such as agricultural residues, industrial processing byproducts, sewage sludge, and animal manure, in an environment devoid of oxygen or with limited oxygen, at temperatures not exceeding 1000 °C, as shown in Fig. 1 [15–17]. Traditionally used in agriculture as soil amendments, biochar has gained attention for its multifaceted applications especially for environmental remediation [18,19]. One of the key advantages of biochar is its high adsorption capacity, owing to its large specific surface area and porous structure. These properties make biochar particularly effective for the adsorption of heavy metals and toxic elements from contaminated soil and water [20]. Biochar is sourced from a variety of renewable biomass wastes, making it a sustainable and low-cost alternative to other remediation materials [21,22]. However, the use of biochar has several challenges. While it offers a cost-effective and environmentally friendly solution, its efficiency in remediating high-concentration contaminants has yet to be fully satisfying. Moreover, the application of large amounts of biochar can sometimes lead to soil nutrient imbalances, requiring careful consideration of its use in different environmental settings. Pristine biochar has its own limitations, one of which is its relatively low adsorption capability for heavy metals and toxic elements. This has led to the exploration of various modification strategies aiming at enhancing its adsorptive properties. These include changing surface charges of biochar using metal nanoparticles, expanding its specific surface area through activating agents, and incorporating metals or metal oxides that can interact with pollutants [23–25].

The advent of nanotechnology and the use of nanomaterials have opened new avenues to enhance the effectiveness of pristine biochar. Incorporating metal nanoparticles (MNPs) into biochar, resulting in biochar-MNPs, is a promising approach to improve its ability to absorb and remove contaminants [26,27]. Nanostructured materials consist of a broad category of substances that have at least one dimension measuring at the nanometer scale. These materials possess structural characteristics that fall somewhere between those of bulk solids and molecules. As a result, they display unique physical, optical, and chemical properties distinct from those of their larger or macroscopic counterparts [28,29]. By incorporating nanoparticles into the biochar matrix, researchers have been able to create a material with synergistic properties that far exceed those of pristine biochar. The nanoparticles can serve multiple functions in this hybrid material. They can increase the surface area and porosity of the biochar, thereby enhancing its adsorption capacity. Additionally, nanoparticles can introduce new functional groups to the biochar, increasing its chemical reactivity, and enabling more effective binding with heavy metals and toxic elements. These nanoparticles, due to their large surface-to-volume ratios compared with the bulk materials, are highly effective against a wide range of pollutants, especially heavy metals and organic compounds [30]. However, they tend to clump together into larger particles, reducing their effectiveness [31]. To address this, biochar has emerged as a popular supporting material for these nanoparticles, given its high surface area and ion-exchange capacities [32,33]. Combining biochar with metal nanoparticles creates a novel composite which maximizes the benefits of both materials while minimizing their drawbacks. Such composites not only stabilize the nanoparticles but also enhance their functional properties. Additionally, nanomaterial-modified biochar has the potential to improve air quality by reducing emissions of harmful gases, such as NOx and VOCs, through enhanced adsorption and catalytic processes. Furthermore, it can contribute to mitigating greenhouse gases by sequestering CO_2 and reducing CH_4 emissions [34]. Biochar's ability to adsorb air pollutants is influenced by its physiochemical properties, such as surface area and functional groups, which can be enhanced through various activation processes and pyrolysis conditions.

This review aims to cover the synthesis techniques for biochar-assisted nanomaterials and their applications in the removal of

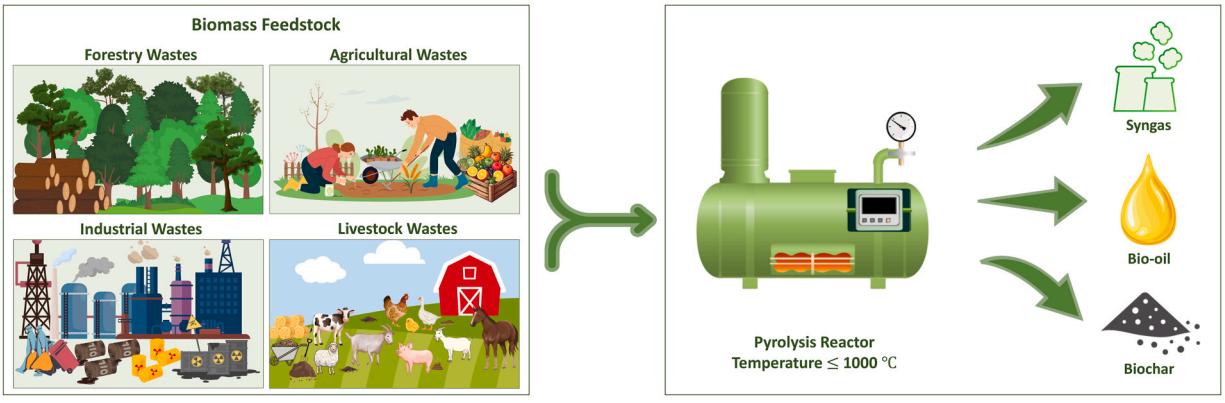

Fig. 1. Feedstocks and pyrolytic outputs of biochar.

various contaminants from the environment. We also discuss the mechanisms behind their effectiveness and suggest directions for future research. Additionally, we explore the potential of these materials to enhance air quality and reduce greenhouse gas emissions, and offer insights into their multifaceted role in environmental remediation and sustainable practices.

2. Nano-modified biochar preparation techniques

Extensive research has been conducted to couple the benefits of biochar's porous structure with the unique physical attributes of nanomaterials, thereby enhancing its capacity to remove both organic and inorganic contaminants. Two primary approaches exist for creating nano-modified biochar with advanced functionalities as depicted in Fig. 2: one involves modifying the initial biomass before its conversion into biochar through processes like pyrolysis, calcination, or coprecipitation; the other one directly alters the already prepared biochar [31,35–37]. These modifications often include surface treatments using various metal precursors, nanoparticles, and organic-inorganic polymers, resulting in biochar nanohybrids. The properties of these biochar-MNPs are influenced by type of feedstock, pyrolysis temperature, ratio of biochar to metal nanoparticles, and pyrolytic reaction media. The modifications often aim to maximize biochar yields by optimizing temperature, heating rate, and residence time based on specific feedstock characteristics [38,39]. The specific surface area (SSA) values for most nano-modified biochars range significantly, from 5.58 to 1736 m^2/g, attributed to their small particle sizes. Research indicates that nano-modified biochar's SSA can rise with an increase in pyrolysis temperature. However, there are different views, with some suggesting that an increase in pyrolysis temperature does not impact or could even decrease the SSA of nano-modified biochars. These discrepancies could stem from variations in the original materials used to produce the nano-modified biochars [40]. Enhancing biochar/biochar-MNPs stability involves post-pyrolysis treatments such as chemical regeneration or physical modification, which not only increase its resistance to degradation but also its efficacy in environmental applications. Chemical regeneration is a key method for reactivating biochar, especially for adsorbing heavy metals and organic pollutants like dyes and antibiotics. The process typically employs solvents and chemical reagents to desorb these pollutants. The efficiency of regeneration depends on the type of pollutants, and different solvents are used for organic and inorganic adsorbates. For instance, in a study involving the removal of lead from wastewater, biochar was regenerated using solutions like sodium hydroxide and hydrochloric acid. The removal efficiency varied across different cycles, generally showing a slight decrease in efficiency over successive cycles. This method ensures biochar maintains its adsorption activity, making it a sustainable option for wastewater treatment [41].

2.1. Biomass modification

Biomass pretreatment entails altering raw feedstock before it is converted into biochar through processes like pyrolysis and calcination. This approach is considered energy-efficient because it allows for the simultaneous processing of both the biomass and metal-containing precursors. During such alteration processes, the original biomass may be subjected to surface modifications using a range of metal-containing compounds, specifically metal oxides, metal chlorides, metal sulfides, metal sulfates, and metal nitrates, along with nanoparticles and organic-inorganic polymers. These modifications facilitate the creation of biochar-supported nanomaterials, the details of which are elaborated in the following section.

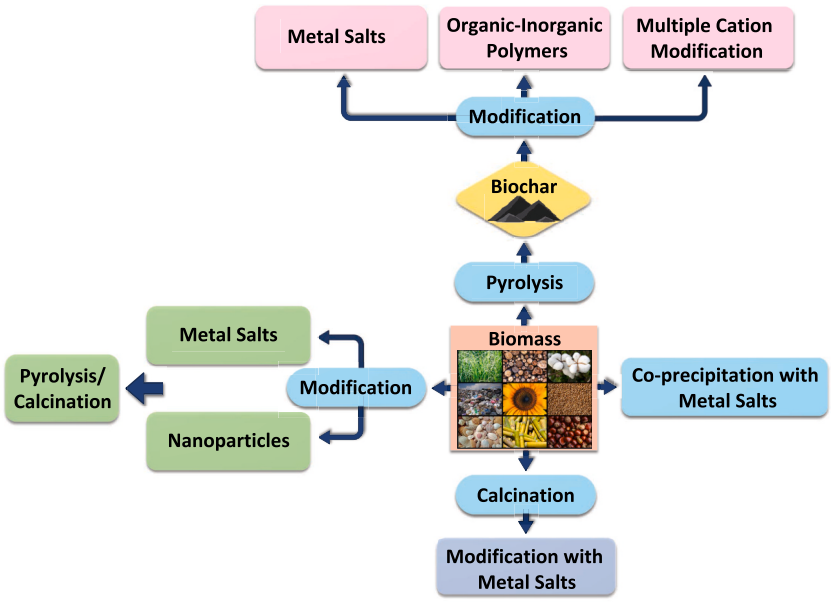

Fig. 2. Schematic diagram of different modification techniques to prepare nano-modified biochar.

Using metal salts to pretreat biomass prior to pyrolysis is a technique for generating biochar-MNPs. Biomass can be impregnated with various metal salts like $FeCl_3$, $Fe(NO_3)_3$, $AlCl_3$, $MgCl_2$, $MnCl_2$, $CaCl_2$, and $ZnCl_2$, as well as sulfur-based and organic-based metal salt solutions, either with or without the application of an electric field [42–46]. This allows metal ions in the solutions to deposit onto the surface or interior of the feedstocks. Following this, the pretreated biomass undergoes pyrolysis at temperatures ranging from 400 to 800 °C in an environment with limited or no oxygen. During the pyrolysis process, these metal ions transform into metal oxide nanoparticles like Fe_2O_3, Al_2O_3, MgO, MnO_2, CaO, and ZnO, or into zero-valent metals that adhere to the biochar surface. For example, in a study reported by Chaukura et al. [47], Fe_2O_3-biochar nano-composite was prepared by pyrolyzing $FeCl_3$-impregnated paper and paper sludge (PPS) at 750 °C. The PPS biomass was immersed in a $FeCl_3$ solution for 2 h and then air-dried at 80 °C for another 2 h. The $FeCl_3$-impregnated PPS, with a mass-to-volume ratio of 1:3, was pyrolyzed at 750 °C for 2 h in a N_2 atmosphere, yielding Fe_2O_3--biochar. This nanocomposite was used for the efficient removal of methyl orange (MO) from contaminated wastewater and the results showed that its MO adsorption capacity was 52.79% higher than that of pristine biochar. The surface area and porosity measured by the Brunauer–Emmett–Teller (BET) method were lower for the Fe_2O_3-biochar composite compared to the pristine biochar. This decrease could be linked to the clogging of the biochar's pores by Fe_2O_3 and other inherent metallic compounds in the absorbent material. Similarly, Fe_3O_4-based magnetic biochar was synthesized by pyrolyzing $FeCl_3$-treated corn straw under an electric field at 600 °C for 1 h. This process resulted in the formation of uniformly dispersed, rod-like Fe_3O_4 nanoparticles on the biochar's surface. Notably, the Fe_3O_4-based magnetic biochar demonstrated a remarkable capacity (113 mg/g) for adsorbing lead [48]. Bismuth-impregnated biochar was produced through the thermal pyrolysis of bismuth oxide and hydrochloric acid-treated wheat straw, at temperatures ranging from 400 to 600 °C [49]. This process, conducted at a heating rate of 10°C/min in a N_2 atmosphere for 1 h, resulted in biochar with a unique porous structure, featuring pores ranging from 0.5 to 1 μm in diameter. This bismuth-modified biochar was noted for its high capacity in adsorbing phosphorus (125.40 mg/g), arsenic (16.21 mg/g), and chromium (12.23 mg/g). This study investigated the use of bamboo biochar, functionalized with Mg-Al and Mg-Fe layered double hydroxides (LDHs), for the efficient removal of phosphate from aqueous solutions. The composite containing 40% Mg–Al LDH exhibited the highest phosphate adsorption, achieving over 95% saturation within 1 h. The research highlighted the potential of using such biochar composites not only for effective wastewater treatment but also as a recyclable material for agricultural applications, promoting sustainable environmental management. In another study reported by Omidvar-Hosseini et al., $Ni_{0.5}Zn_{0.5}Fe_2O_4$ magnetic nanoparticles supported on Acacia Nilotica seed shell ash (ANSA) were synthesized and applied for effective adsorption of Pb(II) ions from water [50]. An aqueous mixture of metal nitrates $Fe(NO_3)_3{\cdot}9H_2O$, $Zn(NO_3)_2{\cdot}6H_2O$, $Ni(NO_3)_2{\cdot}6H_2O$, and ANSA was dissolved in DI water, to which extracted egg-white solution was added. Following 30 min of continuous stirring, the sol-gel obtained was dried at 80 °C to yield dry precursors. These precursors were then finely ground and calcined at 550 °C for 2 h in a muffle furnace. Various characterization techniques like Fourier Transform Infrared Spectrometry (FTIR), Scanning Electron Microscopy (SEM), X-ray Diffraction (XRD), and Vibrating Sample Magnetometer (VSM) confirmed the successful incorporation of nanoparticles into ANSA, forming less than 100 nm particles with superparamagnetic behavior. The Langmuir model best described the adsorption process, and the kinetics fit the pseudo-second-order rate equation. The nanoparticles could be easily separated from water using an external magnet, making them a practical and eco-friendly solution for treating water pollution caused by Pb (II) ions. Similarly, Li group synthesized nano ZnO/ZnS-modified biochar via slow pyrolysis of zinc-contaminated corn stover biomass [46]. Slow pyrolysis was conducted in a lab-scale fixed-bed reactor, using zinc-loaded biomass in a horizontal tubular reactor (60 mm I.D., 300 mm length). The reactor was first purged with N_2 gas to eliminate O_2. Biochar from raw corn stover was then produced at four different temperatures: 500, 600, 700, and 800 °C. This modified biochar, uniformly coated with nano ZnO/ZnS, displayed superior porosity (with a BET surface area of 397.4 m^2/g and a total pore volume of 0.43 cm^3/g) when compared to the unmodified biochar (with a BET surface area of 102.9 m^2/g and a total pore volume of 0.20 cm^3/g). Batch adsorption tests indicate that the obtained biochar modified with nano ZnO/ZnS exhibited a robust ability to absorb Pb (II), Cu (II), and Cr (VI), with maximum adsorption capacities that were notably greater than those of common biochar. Biochar impregnated with magnesium was prepared by pyrolyzing biomass feedstock (cow dung) and utilized to reduce the leaching of phosphorus from the soil [51]. The cow dung biomass mixed with $MgCl_2{\cdot}6H_2O$ solution was placed in porcelain crucibles, which were then sealed and pyrolyzed at 600 °C for 1 h in an O_2-limited muffle furnace. This process was aimed at producing Mg-modified biochar. The data revealed that nanoscale magnesium oxides were uniformly distributed on the biochar's surface. The MgO-biochar composite had a mesoporous structure with an average pore size of 1.74 μm and could effectively minimize the loss of phosphorus through leaching from the soil and offer improved stability.

Using a low-temperature method, coprecipitation of biomass and metal salts can serve as another technique for modifying char. A study by Gupta and colleagues introduced a feasible way to alter the surface of orange peel powder (OPP) by coprecipitating it with ferric chloride hexahydrate and ferrous sulfate heptahydrate. This led to the creation of a novel magnetic nano-adsorbent Fe_3O_4-OPP (MNP−OPP), which showed the covalent binding between the hydroxyl groups in MNP and the carboxyl groups in OPP. The nano-composite was further used for cadmium ion removal from aqueous solutions [52]. It showed that under optimal conditions MNP-OPP achieved a maximum removal of Cd^{2+} at 76.92 mg/g based on Langmuir Model and the adsorption was thermodynamically favorable.

Another approach for creating biochar-MNPs involved directly subjecting biomass rich in target metal elements to pyrolysis. This process transformed the metal elements in the biomass into metal nanoparticles. For instance, biochar rich in calcium (CRB) was prepared by carbonizing crab shells at a temperature ranging from 300 to 900 °C at a heating rate of 10 °C/min for 2 h [53]. Elemental analysis showed a high calcium content, but low carbon content in the crab shell biochar. TG indicated that calcite-based CRB was formed at 600 °C, while lime-based CRB was generated at 700 °C. The nanocomposites showed the phosphorus adsorption efficiency varied from 26% to 100% for a phosphate solution (80 mg/L) and from 11% to 63% for anaerobic digestion effluent. These findings suggest that CRB was effective for removing or recovering phosphorus from wastewater.

In addition to the use of metal oxides/salts, biochar coated with multi-walled carbon nanotubes (CNT) was also reported [54].

Biochar-CNT was produced through slow pyrolysis of carboxyl-functionalized CNT-impregnated feedstocks, including milled hickory chips and sugarcane bagasse. These CNT-treated feedstocks were placed in a quartz tube within a tubular furnace (MTI, Richmond, CA) and subjected to pyrolysis at 600 °C for 1 h, with a heating rate of 10 °C/min, in a N_2-rich environment. It was found that CNTs improved the biochar's physicochemical attributes, such as surface area, porosity, and thermal stability. Batch sorption tests on methylene blue showed efficient adsorption.

Recent studies have increasingly explored the calcination of biomass for biochar and composite material synthesis. This process involves heating inorganic materials to high temperatures to improve crystallinity and remove surface impurities and volatiles. An example of this is the successful synthesis of the sugarcane bagasse-Fe_3O_4 composite through coprecipitation of sugarcane bagasse with $FeSO_4{\cdot}7H_2O$ and $FeCl_3{\cdot}6H_2O$ in the presence of ammonia, followed by calcination [55]. TEM identified spherical or rod-shaped structures in the altered bagasse. A shift in the IR spectrum peak from 897 cm^{-1} to 874.6 cm^{-1} verified the interaction between bagasse and Fe-OH, while the appearance of Fe-O vibration bands confirmed the composite's formation. Furthermore, absorption bands at 712.2 cm^{-1}, 585.5 cm^{-1}, and 436.9 cm^{-1} were attributed to Fe-O vibrations, a consequence of high-temperature calcination.

Table 1 summarizes the various biomass modifications discussed in this section, providing a comprehensive overview of the feedstocks used, the types of metal precursors involved, the conditions under which pyrolysis or calcination was carried out, the specific nanocomposites formed, and their respective applications. This summary table serves as a quick reference for understanding the diversity of approaches in biomass modification for environmental remediation and pollution control, highlighting the efficiency of each method in creating effective nanocomposites for targeted applications.

Table 1
Summary of biomass modifications for metal nanocomposite synthesis and applications.

Feedstock	Metal/Organic or Inorganic Precursor	Pyrolysis Condition	Formed Nanocomposite	Application	Adsorption Efficiency	Adsorption Capacity	Ref
Corn stalk	$FeCl_3$ pretreatment in an electric field	600 °C	EC-Fe_3O_4-biochar	Adsorption of Pb (II) ions from wastewater	/	113 mg/g	[48]
Wheat straw	Bi_2O_3 and hydrochloric acid	400–600 °C	Bismuth-impregnated biochar	Adsorption of P, As (III), and Cr(VI)	/	P = 125.40 mg/g As(III) = 16.21 mg/g Cr(VI) = 12.23 mg/g	[49]
Paper and paper sludge (PPS)	$FeCl_3$	750 °C	Fe_2O_3-biochar	Removal of methyl orange (MO) from contaminated wastewater	52.79% higher than that of pristine biochar	20.53 mg/g	[47]
Acacia Nilotica seed shell ash (ANSA)	Nickel and zinc salts	550 °C	$Ni_{0.5}Zn_{0.5}Fe_2O_4$ on ANSA	Adsorption of Pb (II) ions from water	94.8%, using 0.05 g of adsorbent and 50 mg/L Pb (II)	maximum monolayer adsorption capacity of 37.6 mg/g	[50]
Zinc-contaminated corn stover biomass	Zinc compounds	Slow pyrolysis (different temperatures: 500, 600, 700, and 800 °C)	ZnO/ZnS-modified biochar	Adsorption of Pb (II), Cu(II), and Cr (VI)	~99%	Pb(II) = 135.8 mg/g Cu(II) = 91.2 mg/g Cr(VI) = 24.5 mg/g	[46]
Cow dung	Magnesium	600 °C	MgO-biochar Composite	Reduce leaching of phosphorus from soil	89.25%	30 mg/g	[51]
Orange peel powder (OPP)	Ferric chloride hexahydrate and ferrous sulfate heptahydrate	Coprecipitation (low-temperature method)	Fe_3O_4−OPP (MNP−OPP)	Removal of cadmium ions from aqueous solutions	82%	76.92 mg/g	[52]
Crab shells	Naturally present calcium in crab shells	300–900 °C	Calcite-based and lime-based CRB	Phosphorus removal or recovery from wastewater	26%–100% for a phosphate solution 1%–63% for anaerobic digestion effluent	/	[53]
Carboxyl-functionalized CNT-impregnated biochar	Carbon nanotubes (CNT)	Slow pyrolysis (600 °C)	biochar-CNT	Sorption of methylene blue	47%–64%	2.4 mg/g for HC-CNT-1% 5.5 mg/g for biochar-CNT-1%	[54]

2.2. Biochar modification

2.2.1. Modification using metal precursors

The common approach to acquire biochar-MNPs is enhancing the surface chemistry of biochar through modification with metal precursors. Initially, biomass undergoes transformation into biochar through processes like pyrolysis, hydrothermal carbonization, and gasification. Following this, the biochar is immersed in solutions of metal salts, allowing metal ions to adhere to the biochar's pores and surface. Ultimately, through processes such as coprecipitation, pyrolysis, and pH adjustment, metal nanoparticles are deposited onto the biochar's surface, creating biochar-MNPs. The incorporation of metallic entities into the carbon matrix of biochar not only enhances its surface properties but also facilitates the easier recovery of the adsorbent material after use. For instance, manganese dioxide nanoparticles were loaded onto biochar derived from pyrolyzed invasive water hyacinth using a redox precipitation method, yielding MnO_2-biochar effective for the adsorption of Cd (II), Cu (II), Zn (II), and Pb (II) [56]. Compared to biochar alone, which showed negligible adsorption of heavy metal ions, the MnO_2-biochar nanocomposite demonstrated substantial capacity for adsorbing these ions. Similarly, the coprecipitation process involving the ethanol-mediated reduction of $KMnO_4$ in a biochar suspension led to the creation of the MnO_2-biochar nanocomposite with enhanced porosity [57]. The pore volume of this nanocomposite was approximately three times smaller than that of biochar and 1.5 times smaller than that of nano MnO_2. In a study, sewage sludge-derived biochar was first produced by pyrolyzing the sludge at 600 °C for 3 h at a 10 °C/min heating rate in a N_2 atmosphere. Subsequently, zero-valent iron nanoparticles were immobilized to the biochar, creating SSB-nZVI-biochar [58]. This composite showed remarkable efficiency in removing Cr^{6+} and Pb^{2+} ions from solutions, achieving approximately 90% and 82% removal within 30 min for Cr^{6+} and Pb^{2+}, respectively. Kim et al. modified the Miscanthus biochar with amorphous iron (hydr)oxide to remove arsenite from water [59]. Miscanthus was initially pyrolyzed at 500 °C for 1 h, using a 10 °C/min heating rate in a N_2 atmosphere to produce biochar. Then, to prepare Fe-modified biochar, Fe ions were precipitated onto the biochar by adjusting the pH to 9 using NaOH. This Fe-modified biochar demonstrated enhanced effectiveness in adsorbing arsenite (56.06 and 47.90 mg/g Fe for powder and beads, respectively). In their research, Wan et al. utilized bamboo biochar, which was pyrolyzed at 600 °C for 2 h subsequently functionalized with Mg-Al and Mg-Fe layered double hydroxides (LDHs), to effectively remove phosphate from water solutions [60]. The composite containing 40% Mg–Al LDH exhibited the highest phosphate adsorption, achieving over 95% saturation within 1 h. Tomczyk et al. modified sunflower husk biochar with AgNPs for efficient tetracycline removal [61]. In another study, they effectively created a new electrochemical sensor for the detection of nitrite, achieved by immobilizing gold nanoparticles to biochar [62]. The resulting biochar/Au composite displayed distinctive characteristics, including a vast surface area, numerous surface functional groups, and outstanding conductivity, all contributing to the enhanced performance of the modified fluorine-doped Titanium oxide electrode in sensing applications. Wang et al. developed a biochar derived from the seedling of white myoga ginger decorated with gold nanoparticles (W-biochar/Au) [63]. The as-prepared W-biochar was mixed into the AuNPs colloidal solution and then subjected to pyrolysis again at a specific temperature (700, 850, or 950 °C) for 2 h. This process resulted in the formation of the W-biochar/Au nanocomposite. The nanocomposite formed at 850 °C, was employed for the detection of hydroquinone and catechol, demonstrating extremely low detection thresholds and enhanced sensitivities. This nanocomposite displayed a highly porous configuration, excellent water dispersibility, and an extensive specific surface area. The notable performance of the W-biochar/Au nanocomposite is likely attributed to its pronounced porous architecture and increased relative contents of C-O/N-O, C=O, and COOH/COOR bonds. Zhu et al. developed biochar decorated with magnetic nanoscale zero-valent iron (nZVI-biochars), featuring varying Fe/biochar impregnation ratios [64]. By systematically analyzing the mechanisms involved in the removal of heavy metals, they conclusively demonstrated that nZVI-biochar had superior removal efficiency for various heavy metals (Pb^{2+}, Cd^{2+}, Cr^{6+}, Cu^{2+}, Ni^{2+}, Zn^{2+}). The commendable magnetic properties of the developed material facilitate the easy recycling of nZVI-biochar from wastewater. In a study by Liao et al. pineapple peel waste-based biochar is decorated with both magnetic Fe_2O_3 and lanthanum hydroxide ($La(OH)_3$) and used as phosphate absorbent [65]. As $La(OH)_3$ loading in the composite was increased, the adsorption capacity for phosphate was increased up to 101.16 mg/g although its magnetic property was reduced. The $La(OH)_3$-modified magnetic biochar had an adsorption capacity 27 times greater than that of pristine biochar and substantially surpassed most phosphate adsorbents in capacity. Table 2 presents a comprehensive overview of modified biochar nanocomposites, delineating their feedstock sources, metal precursors used for modification, the pyrolysis techniques employed, and their subsequent applications for environmental remediation.

2.2.2. Other modification techniques

Another method of fabricating biochar involves impregnating biochar with various organic or inorganic polymers. This process transforms the biochar into an effective composite, enhancing its porosity and interface chemistry with heavy metal pollutants. For instance, a bionanocomposite, consisting of an organic-inorganic blend of chitosan, nanoclay, and bark chip-derived biochar, was selected for the simultaneous immobilization of Cu, Pb, and Zn metal ions in contaminated soil and water environments [66]. This bionanocomposite was prepared by adding bark chip-derived biochar to the mixture of nanoclay/chitosan solution. The composite showed a mixed exfoliated/intercalated morphology with the incorporation of minimal nanoclay amounts (5 wt%). The batch adsorption tests revealed that the nanocomposite's adsorption capabilities for Cu^{2+}, Pb^{2+}, and Zn^{2+} significantly surpassed those of the unmodified biochar. As per the FTIR analysis, the predominant mechanism for metal immobilization is interaction with $–NH_2$ groups. Chitosan was utilized as an organic polymer due to its potential biocompatibility, environmental friendliness, and its appropriateness for biocomposite preparation [67]. Nanoclay, with its exchangeable hydrated cations in a layered structure, is commonly applied as an additive to enhance various physical and adsorptive properties of polymers like chitosan [68].

During the preparation of bulk biochar, nanobiochar inherently forms, though its yield is minimal (e.g., ~2.0% in peanut shell biochar) [69]. To enhance the nanoparticle content in biochar, a process for a size reduction is essential, which can be conducted

Table 2
Overview of modified biochar nanocomposites: feedstock sources, metal precursors, pyrolysis techniques, and remediation applications.

Feedstock	Metal/Organic or Inorganic Precursor	Pyrolysis Condition	Formed Nanocomposite	Application	Adsorption Efficiency	Adsorption Capacity	Ref
Invasive water hyacinth	Manganese Dioxide	Slow pyrolysis at low temperature (450 °C)	MnO_2-biochar	Adsorption of Cd(II), Cu(II), Zn (II), Pb(II)	/	Cd (II) = 232.5 mg/g Cu (II) = 248.9 mg/g Zn (II) = 239.4 mg/g Pb (II) = 249.2 mg/g	[56]
Sewage sludge	Zero-Valent Iron	600 °C for 3 h, 10 °C/min in N_2 atmosphere	SSB-nZVI	Removal of Cr^{6+} and Pb^{2+} ions	Cr^{6+} = 90% Pb^{2+} = 82%	/	[58]
Miscanthus	Amorphous Iron (hydr)oxide	500 °C for 1 h, 10 °C/min in a N_2 atmosphere	Fe-modified biochar	Arsenite adsorption	/	Arsenite powder = 56.06 mg/g Arsenite beads = 47.90 mg/g	[59]
Bamboo	Mg-Al and Mg-Fe LDHs	600 °C for 2 h	Mg-Al/Mg-Fe LDH-modified biochar	Phosphate removal from water	95%	Mg-Fe LDH (40%)/biochar = 7.58 mg/g Mg-Al LDH (40%)/biochar = 13.11 mg/g	[60]
Sunflower husk	Silver Nanoparticles (AgNPs)	650 °C	AgNPs-Modified biochar	Tetracycline removal	42.04%	9.55 mg/g	[61]
Tea waste	Gold Nanoparticles (AuNPs)	500 °C for 2 h	biochar/Au Composite	Electrochemical sensor for nitrite detection	~100%	/	[62]
White myoga ginger (W)	Gold Nanoparticles (AuNPs)	700, 850, and 950 °C for 2 h	W-biochar/Au	Detection of hydroquinone and catechol	~95–100%	/	[63]
Wetland plant Reed	$FeCl_3$	600 °C for 90 min	nZVIr-biochar	Removal of Pb^{2+}, Cd^{2+}, Cr^{6+}, Cu^{2+}, Ni^{2+}, and Zn^{2+} from polluted water sources	Pb^{2+}, Cu^{2+}, Cd^{2+}, Ni^{2+}, and Zn^{2+} > 98% Cr^{6+} = 48.9%	Pb^{2+} = 38.31 mg/g Cu^{2+} = 30.37 mg/g Cr^{6+} = 23.09 mg/g Cd^{2+} = 39.53 mg/g Ni^{2+} = 47.85 mg/g	[64]
Pineapple peel waste	Fe_2O_3, Lanthanum Hydroxide ($La(OH)_3$)	300 °C	Magnetic biochar with La $(OH)_3$	Phosphate adsorption	>96.04%	101.16 mg/g	[65]
Bark chips	Chitosan and nanoclay	600 °C at 10 °C/min and 2 h residence time under N_2 flow	Organic-inorganic composite of chitosan, nanoclay, and biochar	Immobilization of Cu, Pb, and Zn	MTCB reduces the metal leaching from the soil by 100, 100, and 52.29% for Cu^{2+}, Zn^{2+}, and Pb^{2+}, respectively	Cu^{2+} = 121.5 mg/g Pb^{2+} = 336 mg/g Zn^{2+} = 134.6 mg/g	[66]
Waste pinus needles (*Pinus roxburrghii*)	$FeCl_3$/g-C_3N_4/$FeVO_4$	600 °C at 10 °C/min	g-C_3N_4/$FeVO_4$/Fe@NH_2-biochar	Removal of methyl paraben (MeP) and 2-chlorophenol (2-CP)	98.4% degradation of MeP 90.7% degradation of 2-CP	/	[74]
Sawdust	Ag/Fe Nanoparticles	500 °C	biochar-supported Ag/Fe nanoparticles (Ag/Fe/MB)	Removal of cephalexin from aqueous solution	More than 86% of CLX was removed by Ag/Fe/MB in 90 min	/	[75]

effortlessly through grinding or milling. Previous studies have employed hand grinding with mortars to decrease the size of various bulk biochars [70]. Ball milling has been underscored as a promising method to boost the yield and reduce the particle size of nano-modified biochar for large-scale production [71,72]. Key ball milling parameters include ball diameters, ball-to-biochar mass ratio, milling speed, duration of milling, temperature, and liquid media [73].

While nano-modified biochars have demonstrated improved adsorption properties, it is anticipated that the incorporation of a multi-cationic salt can further enhance adsorption by introducing a dual adsorption mechanism to the biochar. For example, in a study, g-C_3N_4/$FeVO_4$ (CI) and g-C_3N_4/$FeVO_4$/Fe@NH_2-biochar (CIB) nano-hetero assemblies were synthesized for the removal of methyl paraben (MeP) and 2-chlorophenol (2-CP) using a combination of adsorption photocatalysis and photo-ozonation [74]. The study demonstrated excellent results, achieving 98.4% degradation of MeP and 90.7% degradation of 2-CP under simultaneous adsorption and photocatalysis in the presence of CIB. In their research, Wu et al. developed biochar-supported Ag/Fe nanoparticles (Ag/Fe/MB) for the removal of cephalexin (CLX) in aqueous solution. The process involved synthesizing nano zerovalent iron (nZVI) on biochar using $FeSO_4 \cdot 7H_2O$ and $NaBH_4$. This was then treated with $AgNO_3$ under vigorous stirring, leading to the formation of a discontinuous Ag layer on the nZVI/biochar surface. The Ag/Fe/MB composite was highly effective in removing CLX from aqueous solution. Specifically, it was found that more than 86% of CLX was removed by Ag/Fe/MB in 90 min under the conditions of 1.5 g/L Ag/Fe/MB dose, CLX initial concentration of 20 mg/L, and a pH of 6.15 [75].

2.3. Characterization of surface chemistry and other properties

For a comprehensive understanding of structural features, physicochemical properties, contaminant adsorption mechanisms of biochar-MNPs, it is crucial to apply a series of analytical techniques for extensive characterization as outlined in Fig. 3 and discussed below.

FTIR is a powerful tool for the detailed characterization of pristine and nano-modified biochar, providing insights into their chemical structure, functional groups, and modifications, which are vital for their applications in environmental remediation and other fields. For instance, Zhang et al. employed FTIR to reveal numerous surface functional groups of biochar/Au composite material

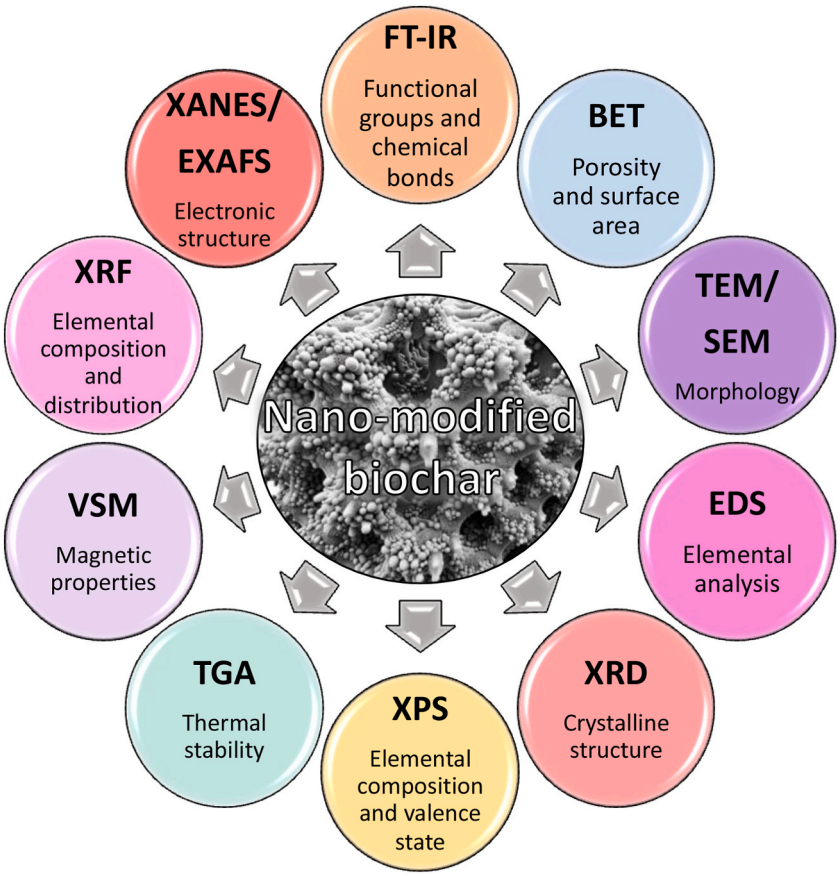

Fig. 3. Characterization techniques for nano-modified biochars. Fourier Transform Infrared Spectrometry (FT-IR), Brunauer–Emmett–Teller (BET) method, Transmission Electron Microscopy (TEM), Scanning Electron Microscopy (SEM), Energy-Dispersive X-ray Spectroscopy (EDS), X-ray Diffraction (XRD), X-ray Photoelectron Spectroscopy (XPS), Thermogravimetric Analysis (TGA), Vibrating Sample Magnetometer (VSM), Confocal Micro X-ray Fluorescence (μ-XRF), X-ray Absorption Near-Edge Structure (XANES), and extended X-ray Absorption Fine Structure (EXAFS).

[62]. The spectral region between 3500 and 3100 cm^{-1} was assigned to the stretching vibrations of O-H (hydrogen bond). Vibrations of C-H stretching (hydrogen bond) were represented in the 3930–2910 cm^{-1} range. The spectral band from 1740 to 1655 cm^{-1} arose due to the stretching vibrations of C=O. The 1280–1210 cm^{-1} region corresponded to the stretching of C–O and the presence of aromatic ring. Lastly, the 1000–650 cm^{-1} range is associated with vibrations of M − O, where M denotes metal or Si. Research on studying functional groups on nano-modified biochars is limited. Biochars are known to have numerous functional groups on their surfaces and display heterogeneous compositions [69]. The surface O/C ratios can undergo substantial modifications, especially at synthesis temperatures between 300 and 400°C, impacting the overall surface behavior, and reactivity [76]. The synthesis temperature is pivotal in determining the surface characteristics of both bulk and nano-modified biochars. Biochar generated at lower temperatures (below 400 °C) experiences less severe carbonization and has a lower degree of aromaticity but more surface functional groups, exhibiting enhanced adsorption capabilities. In contrast, biochars created at elevated temperatures (higher than 700 °C) tend to have reduced functional groups due to the removal of heteroatoms like O, N, and S during the charring process [77]. This leads to the presence of polyaromatic rings (characterized by X-ray adsorption spectroscopy) with various functional groups such as O-, S-, and N-functional entities. The hydrophilic properties and negative charges are predominantly attributed to the O-functional groups such as –OH, –COOH, –C=O, and –C–O, as the deprotonation of these groups results in net negative surfaces [78]. Additionally, nano-modified biochars may incorporate N-H bonds and SiO_2. Comparatively, nano-modified biochars feature both polar and non-polar sites along with a plethora of hydroxyl, carboxylic, and carbonyl functional groups.

The BET method is utilized to ascertain specific surface area and distribution of pore sizes. For example, Zhang et al. used a BET surface analyzer to measure the pore size distribution and surface area of biochar-MnO_2 material [56]. Biochar initially had a minimal BET surface area of 3.5 m^2/g due to its substantial particle size. However, a notable enhancement in its BET surface area was observed upon the deposition of MnO_2. Biochar loaded with varying amounts of MnO_2 displayed superior specific surface areas compared to unmodified biochar, indicating the increase in biochar's specific surface area via post-MnO_2 modification. The specific surface area of biochar-MnO_2 escalated from 135.9 m^2/g to 181.5 m^2/g as the MnO_2 loading amount rose from 12.3% to 18.4%. Conversely, a further increase in MnO_2 loading amount resulted in a decrease in the specific surface area of biochar-MnO_2. The initial enhancement can be attributed to the incorporation of MnO_2 nanoparticles and the formation of additional micropores. The subsequent reduction at elevated loading is presumably due to the excessive deposition of MnO_2 nanoparticles, potentially causing blockage of pores and disruption of certain micropore structures.

Transmission Electron Microscopy (TEM) and SEM are employed to examine the microstructure, morphology, and the dispersion of metal nanoparticles within the biochar-MNPs. For instance, Yang et al. explored the structure and morphology of the biochar/Fe-Mn-S composite utilizing SEM and TEM [79]. SEM imagery revealed that the ternary needle-like Fe-Mn-S mixtures were uniformly distributed on the hierarchical biochar, which possessed numerous regular and vertical channels. TEM images displayed the contours of nanorods, having diameters of several nanometers and lengths varying from several to hundreds of nanometers. Energy-Dispersive X-ray Spectroscopy (EDS) is a technique used for characterizing the elemental composition of materials. If biochar is modified with metal nanoparticles, EDS can be used to confirm the presence of metal elements on the biochar surface and provide information about their concentration and distribution. Wang group adopted EDS to analyze the types and molar fraction of elements in a biochar sample decorated with gold nanoparticles [80]. The distributions of C, O, N, and Au appear to be uniform across the entire surface. Therefore, the combined results from their SEM and EDS analyses, effectively demonstrate the embellishment of biochar with gold nanoparticles. In addition, an elemental analyzer was also used for analyzing C, H, O, and N. Biochar is predominantly composed of those elements, along with varying concentrations of vital mineral nutrients, and exhibits significant diversity in trace elements. The nitrogen component of biochar is influenced by feedstock and pyrolysis temperature. During pyrolysis, peptide bonds transform into N-heteroaromatic carbon compounds [69]. Biochar derived from plants usually possesses a richer mineral content.

XRD is a versatile tool that can provide a wealth of information about the structural and compositional characteristics of pristine and nano-modified biochars. It offers valuable insights into the crystalline nature, mineral content, and other structural attributes of the char by analyzing the diffraction patterns. For instance, Wang et al. employed XRD to examine the crystalline phase and structural characteristics of magnetic nano-modified biochar [81]. The XRD analysis of the magnetic nano-modified biochar revealed peaks at 2θ values of 30.2°, 35.6°, 43.3°, 53.7°, 57.2°, and 62.9°, which correspond to the γ-Fe_2O_3 crystalline phases. Given the similar diffraction peaks of γ-Fe_2O_3 and Fe_3O_4, the XRD results confirmed the formation of both Fe_3O_4 particles within the composite.

X-ray Photoelectron Spectroscopy (XPS) is a surface-sensitive analytical technique that provides information about the elemental composition, chemical state, and electronic state of the elements present in the pristine and nano-modified biochars. In 2019, Yang's group utilized XPS to examine the surface composition and chemical states of a straw biochar functionalized with lanthanum ferrite ($LaFeO_3$) nanoparticles [82]. The observed peaks at 835.0, 836.2, and 839.7 eV for $LaFeO_3$/biochar correspond to the binding energies of La (3d), suggesting that La is predominantly in its oxidized state. For $LaFeO_3$/biochar, the Fe (2p) peaks are located at 711.5 and 725.1 eV, with no discernible shoulder peaks, signifying the Fe ions are in the Fe^{3+} oxidation state. The 529.8 eV peak is attributed to lattice oxygen atoms, specifically La–O and Fe–O in the $LaFeO_3$ crystal structure. Regarding C in $LaFeO_3$/biochar, the C (1s) signal deconvolution revealed the presence of C–C bonds at binding energies of 283.7, 284.7, and 285.1 eV. These data confirm the successful incorporation of $LaFeO_3$ onto the biochar surface.

Thermogravimetric Analysis (TGA) is a thermal analysis technique used to measure the weight change of a sample as a function of temperature or time under a controlled atmosphere. For example, Zhang et al. employed TGA to study the development of MgO-biochar [83]. The TGA curve for sugar beet tailings revealed four distinct weight loss phases. The first phase, from 30 to 200°C, was attributed to the evaporation of residual water molecules. The subsequent phases, from 200–300 °C, 300–400 °C, and 400–550 °C, were attributed to the decomposition of lignin, cellulose, and hemicellulose, respectively. The TGA curve for $MgCl_2$-treated sugar beet tailings also showed four stages. The initial weight loss was due to the water molecule evaporation from 30 to 100 °C. The subsequent

decrease in weight was linked to the breakdown of $MgCl_2$ hydrates from 100 to 250 °C. The third drop in weight was likely due to the formation of magnesium hydroxychloride and the further degradation of hydrates from 250 to 450 °C. The final weight reduction was associated with magnesium oxide formation alongside decomposition of magnesium hydroxychloride from 450 to 650 °C.

VSM provides a comprehensive analysis of the magnetic properties of pristine and nano-modified biochars. For example, Li et al. utilized a vibrating sample magnetometer to assess the magnetic saturation of biochar fabricated with magnesium oxide [84]. The biochar impregnated with magnesium displayed a saturation magnetization of 35.35 emu/g, suggesting it could be readily magnetized. Impressively, even after being submerged in water for five months, this magnesium-impregnated magnetic biochar could be effectively recaptured using a permanent magnet.

In recent years, innovative methods have been employed to analyze multifunctional composites. Techniques like X-ray Absorption Near-Edge Structure (XANES) and the extended X-ray Absorption Fine Structure (EXAFS) are used to provide deep insights into the interaction between the biochar matrix and the nanoparticles, the chemical state of the metals, and the nature of the metal-containing species. Confocal Micro X-ray Fluorescence (μ-XRF) is applied to ascertain the elemental composition and distribution in biochar-MNPs [85]. In a study by Feng et al., they utilized XANES, EXAFS, and μ-XRF to study the characteristics of Fe-biochar [86]. The results from Fe XANES and EXAFS revealed γ-Fe_2O_3 as the dominant Fe species in the composite, with Fe° being detected at temperatures of 600 or 900°C. The μ-XRF analysis highlighted the dispersion of Fe, S, and Cl within the porous structure, with Fe accumulating on the biochar's surface.

3. Multifunctional applications of nano-modified biochar in environmental remediation

Recent studies have delved into the diverse applications of nano-modified biochars, such as catalyst, an alternative for carbon black, biomolecule carrier, and the removal of various contaminants like agrochemicals and pharmaceuticals [73,87–89]. Due to its superior adsorptive properties, nano-modified biochar showcases an impressive ability to adsorb a broad spectrum of contaminants. Moreover, nano-modified biochar can also act as a catalyst, promoting the decomposition of organic compounds [90].

3.1. Heavy metal removal

Heavy metal contamination poses significant environmental threats, impacting both ecosystems and public health. Nano-modified biochar has gained prominence due to its notable reactivity, high surface area, and ion-exchange capabilities, making it effective in the removal of heavy metals like As, Hg, Cr, Cu, Cd, and Pb [91]. Some of these heavy metals are non-essential and known to be detrimental to human health due to their acute and chronic toxic effects. Meanwhile, others are trace elements vital for human well-being but can become harmful if their levels surpass the recommended thresholds [92]. Therefore, effective heavy metal removal strategies including stabilization, microbial remediation, and electrochemical methods are required in agricultural and environmental research. Several factors, including dosage, presence of other ions, initial heavy metal concentration, and pH, influence the nano-modified biochar's performance. The removal processes involve multiple mechanisms, including adsorption, reduction, precipitation, co-precipitation, ion exchange, and oxidation. To elucidate these mechanisms, various analytical techniques as shown in Fig. 3, are employed. The ability of nano-modified biochars to extract heavy metals, the influence of different factors on this removal efficiency, and the underlying mechanisms are comprehensively discussed below.

Numerous studies have demonstrated the effectiveness of nano-modified biochars in removing heavy metals and have assessed their capacity for such removal. To gauge the efficiency of nano-modified biochars in extracting heavy metals, various models such as Langmuir, Freundlich, Langmuir-Freundlich, Temkin, and Sips are used to interpret the collected data. Moreover, models like the first-order kinetic, Elovich, intraparticle diffusion, and second-order kinetic are applied to ascertain the rate of heavy metal removal. In a study by Wan et al., a magnetic biochar, which combines the advantages of both biochar and iron oxides, effectively removed multiple metal(loid) contaminants from the soil [93]. There was a notable reduction in the soil concentrations of As, Cd, and Pb by 28%, 25%, and 32%, respectively, within 24 h. The Fe_3O_4-modified biochar not only removed the soluble and exchangeable fractions of metal (loid)s, but also directly adsorbed the solid fractions. A novel porous biochar activated with K_2CO_3 and infused with nano-zero-valent iron and nano-α-hydroxy-iron oxide was tested for Cd (II) removal from aqueous solution, as reported by Zhu et al. [94]. The Cd (II) adsorption onto this composite was best explained by the pseudo second-order kinetic model, suggesting that chemisorption primarily controlled the process. The composite's adsorption rates for Cd (II) were notably rapid. Furthermore, the Langmuir model provided the most accurate fit for the experimental data. The composites' maximum adsorption capacities for Cd (II) were measured at 26.43 mg/g and 22.37 mg/g. When compared to other materials, these composites demonstrated superior efficacy in removing Cd (II). Nano-modified biochar prepared by ball-milling process was used to remove Ni (II) (a model contaminant) [73]. The results showed that this ball-milled nano-modified biochar was more efficient in Ni (II) removal than the pristine biochar. It also demonstrated rapid adsorption rates and outstanding Ni (II) adsorption capacity, surpassing many commercial sorbents (e.g., Activated carbon, Na-montmorillonite, natural bentonite, and Chlorella sorokiniana). Compared to the pristine biochar, the ball-milled nano-modified biochar exhibited enhanced physical and chemical features, such as increased surface area and more acidic functional groups. As a result, its ability to remove contaminants surpassed that of the pristine biochar.

The effectiveness and stability of heavy metal removal using nano-modified biochars depend on various environmental factors (soil minerals, feedstock, pyrolysis temperature, nanoparticle content, biochar loading, additives, etc.). For instance, when using biochar loaded with polymetallic nanoparticles, the heavy metal immobilization varies based on the nanoparticle to biochar ratio. In a study reported by Zhang et al., they examined how the addition of iron, manganese, and cerium oxide (FMCBC) to biochar affected arsenic availability in arsenic-polluted paddy soil [95]. The FMCBC with different mass ratios of 24:2:3:4 ($FMCBC_1$), 24:2:3:8 ($FMCBC_2$), and

24:2:3:10 ($FMCBC_3$) for biochar, Fe, Mn, and Ce respectively, was used for the polluted soil treatment. The findings indicate that FMCBCs enhance the soil's pH and redox potential, leading to a reduction in the bioavailable arsenic forms. Among all treatments, $FMCBC_3$ had the highest reduction in soil-bound arsenic concentration. The conditions under which pyrolysis is conducted, including temperature and gas flow, influence the functional groups and surface area of biochar composites. For example, greater immobilization of Cr is observed at higher pyrolysis temperatures, specifically at 700 °C, as noted by Rafique et al. [96]. As pyrolysis temperatures rise, functional groups like alcoholic, aliphatic, and ester on the biochar surface diminish, as observed by Shakya et al. [97]. Additionally, hemicellulose breaks down at temperatures above 350 °C, leading to a rapid release of volatile compounds that form pores [98]. As a result, the capacity to immobilize increases with temperature due to enhanced surface area.

3.2. Organic pollutant removal

Nano-modified biochars have also demonstrated a strong adsorption to organic contaminants. Nano-modified biochar serves as an adsorbent, reductant, and catalyst in removing organic contaminants such as persistent organic pollutants, cancer-causing compounds, pesticides, and antibiotics. These applications are relevant to environmental and agricultural settings because of its strong adsorptive, catalytic, and reductive properties. Recent research indicates that carcinogenic persistent organic pollutants (POPs), such as polycyclic aromatic hydrocarbons (PAHs) and polybrominated diphenyl ethers (PBDEs), can make their way to the food chain. Due to their carcinogenic properties (e.g., low solubility, high molecular weight, and persistence), they pose potential threats to both human health and the environment [99,100]. Therefore, nano-modified biochars can serve as an effective tool for removing these pollutants from the environment. For instance, using the liquid phase reduction method, biochar-supported nano zero-valent iron (biochar-nZVI) was synthesized to activate persulfate (PS) for decabromodiphenyl ether (BDE209) removal from soil [101]. The data indicated that at a PS/biochar-nZVI molar ratio of 3:1, pH 3, and 40°C, 82.06% reduction of BDE209 was achieved in 4 h. In another study, biochar nanocomposites modified with copper oxide (CuO) were synthesized for removing anionic contaminants (reactive red RR120) from water [102]. The work highlighted the robust interaction between CuO and biochar. The embedded CuO nanoparticles in the composite demonstrated superior removal of reactive red due to strong electrostatic attraction. The CuO/biochar nanocomposite showcased the best RR120 removal efficiency at 46%, significantly outperforming the original biochar at 20%. Furthermore, the adsorption process was quick, with an equilibrium time of less than 3 h. The impact of different particle sizes (sub-millimeter, micron-scale, and nano-scale) of biochar derived from corn straw and rice husk was studied on the adsorption of diethyl phthalate (DEP) [103]. The findings revealed that the smaller the biochar particle size, the greater its capacity to adsorb DEP, with nano-scale biochar demonstrating the highest adsorption capability. This increased adsorption in nano-scale biochar was due to its advanced pore structure and larger specific surface area. This suggests that nano-scale biochar's DEP adsorption primarily resulted from pore-filling, rather than interactions like π-π EDA and H bonding observed in larger-sized biochar. Moreover, the nano-scale biochar's ability to adsorb DEP significantly dropped when the initial pH value was reduced from 9 to 3. This was because an acidic environment diminished the surface charge on the nano-scale biochar, causing easier agglomeration of the particles. Phthalate esters (PAEs) are commonly used as plasticizers in plastic products worldwide, leading to the potential bioaccumulation of benzene carboxylic groups. It is crucial to remove PAEs from environments like soil and sediment. Two prominent plasticizers, Dibutyl phthalate (DBP) and di-(2-Ethylhexyl) phthalate (DEHP), are prevalent residues in soil and are listed as priority pollutants by the US Environmental Protection Agency. In a study, the impact of using the Fe-Mn oxide-modified biochar composite (FM-biochar) was investigated on the quality of wheat cultivated in brown soil contaminated with DBP and DEHP [104]. Introducing FM-biochar notably reduced the adsorption of DBP and DEHP by wheat grains, leading to enhancements in the grain quality, specifically in starch, protein, and amino acid levels. Moreover, the results from FM-biochar applications surpassed those from biochar treatments, suggesting that FM-biochar is a potent method to lower the bioavailability of PAEs to wheat grains. In their report, Bentley et al. showed improved adsorption capacities for certain organic micropollutants (OMPs) using pine-derived biochars pre-treated with NaOH (pH 9 and 11) and various alkali and alkaline earth metals (AAEMs) like Na, K, Ca, and Mg [105]. This treatment notably increased the surface area of the biochar's micropores, with the most significant improvement observed at pH 11, where the OMP adsorption rate nearly matched that of commercial activated carbon, surpassing untreated biochars. This underscores the effectiveness of specific pre-treatments in enhancing biochar for water treatment applications.

3.3. Nano-modified biochars' role in soil health and air quality

Biochars, as soil amendments, have a significant impact on soil microbial activity, playing a crucial role in enhancing soil health and fertility. Their porous structure and high surface area provide a conducive habitat for diverse microbial communities, facilitating the proliferation of beneficial microorganisms. Biochars are known to influence soil pH, moisture retention, and nutrient availability, all of which are critical factors affecting microbial growth and activity. Notably, they can improve the soil's carbon content, offering a stable carbon source for soil microbes, thus stimulating their metabolic processes. The interaction between biochar and soil microbes often leads to increased soil enzyme activities, indicative of enhanced nutrient cycling and organic matter decomposition. Furthermore, the presence of biochar can help in mitigating the negative effects of soil contaminants, thereby reducing the stress on microbial communities. This, in turn, supports the restoration of microbial diversity and function in degraded soils.

Soil microorganisms play a pivotal role in nutrient cycling, breaking down soil organic matter to release nutrients in accessible forms for plants and other microbes, integral to the soil-plant biogeochemical cycle. Any changes affecting these microbes or nutrient cycling can impact ecosystem functionality. Previous findings indicate that nano-modified biochars can transform the composition of soil microbial communities and influence their metabolic capacity, particularly in nutrient cycles like carbon and nitrogen cycling. The

presence of nano-modified biochars affects enzyme activities, functional genes, and microbial species involved in nitrogen and carbon cycling. Factors such as soil pH, bioavailable metals, and soil electric conductivity (EC) also impact bacterial communities, hindering phototroph growth and leading to a decrease in carbon fixation genes [106]. Additionally, dissolved organic carbon (DOC) released from biochar forms reactive oxygen species, which can damage cellular components of phototrophs, reducing the relative abundance of carbon fixation genes [107]. The promotion of carbon-degrading organisms by MgO-biochar might be associated with increased cellulase activity, releasing more glucose and thereby boosting the abundance of carbon-utilizing bacteria [108]. In some cases, the rise in certain key orders related to carbon-cycling bacteria in modified biochar treatments could regulate the carbon cycle. In general, the use of nano-modified biochars can influence crop growth and yield, affect the behavior and survival of soil fauna, and alter soil properties like pH and organic matter [109]. These changes impact the structure of soil microbial communities, which are crucial for processes like carbon and nitrogen cycling.

Nano-modified biochars have also shown significant potential in improving air quality by reducing emissions of harmful gases such as nitrous oxide (N_2O) and methane (CH_4), and sequestering greenhouse gases like carbon dioxide (CO_2) [110–112]. The high surface area and reactivity of nano-modified biochar enable it to adsorb pollutants more efficiently than conventional biochar. By altering the soil's physicochemical properties, nano-modified biochar enhances its ability to retain and degrade airborne pollutants and provides a more favorable environment for microbial communities that break down these gases. This, in turn, contributes to both improved soil health and air quality by decreasing greenhouse gas emissions through the modification of soil microbial activities that influence the nitrogen and carbon cycles [34].

4. Mechanisms of pollutant removal by nano-modified biochars

As discussed above, nano-modified biochar has been identified as a capable adsorbent for removing specific pollutants, including heavy metals and organic pollutants. Understanding the interaction mechanism between pollutants and nano-modified biochar is vital

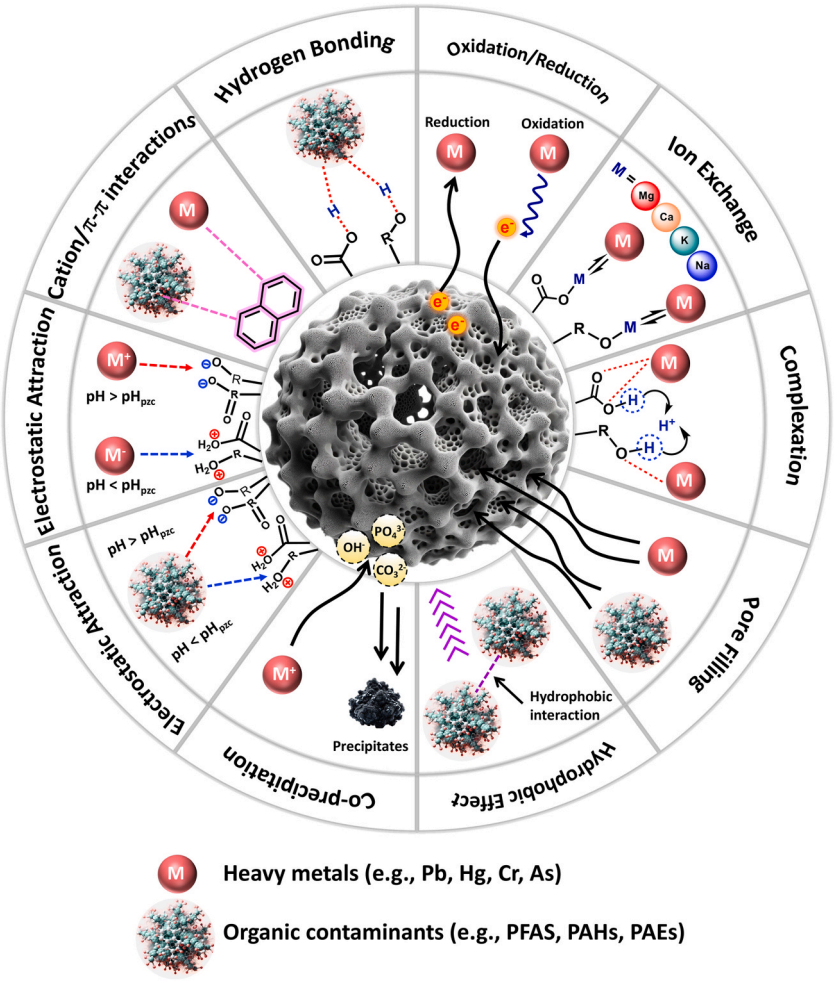

Fig. 4. Interaction mechanism between heavy metals and organic pollutants with biochar particles.

for linking remediation to the engineering design of these materials [113,114]. Factors such as pH and material dosage significantly influence the efficiency of pollutant removal. Extensive research has been carried out to explore the remediation abilities of nano-modified biochar for heavy metals and organic compounds in polluted environments. The proposed mechanisms behind pollutant adsorption are illustrated in Fig. 4 and discussed below.

4.1. Mechanisms involved in metal removal

Electrostatic Interactions. Electrostatic adsorption, which is fundamental to the formation of ionic bonds, can be affected by factors such as point of zero charge (PZC), the pH level, and the heavy metal's ionic and valence radii. In general, elements like chromium, arsenic, and antimony form anionic species in water, and because they are negatively charged, they tend to repel away from the similarly charged surface of unmodified biochar. This electrostatic repulsion limits the capacity of pristine biochar to adsorb these elements. To overcome this limitation, modifications to biochar are often employed to improve its adsorption capabilities. For example, Zhang et al. observed that by loading chitosan into bamboo biochar, the adsorption capacity for hexavalent chromium (Cr (VI)) was significantly enhanced, reaching up to 127 mg/g of biochar. This increase in adsorption was attributed to the electrostatic attraction between the positively charged hydroxyl and amine groups of chitosan and the CrO_4^{2-} ions [115]. Likewise, it was reported that the KOH-modified, nitrogen-enriched biochar (KNB) derived from waste chicken feathers, was effectively utilized for the adsorption of Cd and Pb from wastewater [116]. KOH modification significantly enhanced the adsorption capacities of the biochar. Electrostatic interactions were one of the primary mechanisms for Cd and Pb adsorption by KNB. The modification with KOH enhanced the biochar's surface functional groups, which in turn increased its electronegativity. This enhancement resulted in a stronger electrostatic attraction to Cd and Pb ions.

The adsorption efficiency of engineered biochar for positively charged heavy metals, such as cadmium, lead, copper, zinc, and nickel, is significantly affected by several factors. These factors include the surface area of biochar, its zeta potential, the nature of minerals present in biochar, the types of functional groups on the biochar surface, as well as the conditions present in the solution. For example, FTIR analysis indicated that Cd^{2+} ions were likely adsorbed onto the surface of iron oxide through electrostatic attraction. Furthermore, the analysis suggested that surface complexation occurs between the Cd^{2+} ions and the Fe_3O_4, involving π-orbital bonding of the metal ions to the π-electrons of the carbon atoms on the surface [117].

Complexation. The surfaces of the biochar are enriched with oxygen-containing functional groups such as -OH, -COH, and -COOH. These groups participate in complex formation with metal ions, resulting in the creation of stable metal complexes. For instance, a biochar supported nano-scale zero-valent iron (biochar-CMC-nZVI), which was stabilized with carboxymethyl cellulose (CMC), was utilized for the effective removal of hexavalent chromium (Cr (VI)) from water [118]. The XPS pattern indicated that alcohol, phenolic, aliphatic, and aromatic carbon were present, suggesting that surface complexation played a crucial role in the adsorption process of Cr (VI). The FTIR spectra of the composite post-reaction revealed alterations in the Fe–O, C–O, and O–C=O groups, indicating that complexation and electrostatic attraction occurred between Cr (VI) and the composite's iron-containing functional groups. Also, various materials such as metal oxides, sulfides, and carbon-based nanomaterials have been utilized to enhance biochar for the purpose of extracting Sb from water [119,120]. In a specific instance, Wang et al. developed biochar infused with lanthanum (La) that possessed magnetic properties [121]. This modification significantly boosted its capacity to adsorb Sb(V), with the adsorption capacity rising from 2.2 to 18.9 mg/g at a neutral pH of 7. Characterization using FTIR and XPS techniques indicated that the primary mechanism behind the improved adsorption of Sb(V) was the formation of a stable inner-sphere La–O–Sb complex within the material's structure.

Ion Exchange. Ion exchange involves the selective exchange of exchangeable metal ions like K^+, Mg^{2+}, Na^+, and Ca^{2+} on the biochar surface with other metal ions. This process is largely influenced by the chemical characteristics of the biochar's surface [122]. The investigation into the mechanism behind Cu (II) removal by Fe_3O_4-alginate modified biochar involved characterizing the composite post Cu (II) adsorption using FTIR and XPS techniques [123]. Shifts and changes in the FTIR spectral adsorption peaks after Cu (II) adsorption suggested interactions between Cu (II) and the composite's functional groups. Moreover, notable shifts in the Cu 2p and Fe 2p peaks in the XPS spectrum after Cu (II) adsorption indicated that ion exchange took place between Cu (II), the composite material, and Fe_3O_4.

Redox Reactions. Some biochars may facilitate redox reactions due to the presence of electron-donating or accepting sites. This can transform the metal ions into a less mobile and less toxic state [124]. For example, an iron-enhanced biochar was utilized to assess the adsorption capacity of As, Cd, and Pb by rice crops. Heavy metals, particularly arsenic in the forms of As (III) and As (V), undergo redox reactions on the surface of biochar due to the strong oxidizing and reducing agents present, resulting in the formation of stable inner-sphere complexation of As on the biochar surface [125].

Precipitation. Biochar can co-precipitate with heavy metal cations, forming insoluble carbonates and phosphates that serve to immobilize heavy metals in soils. Liang et al. enhanced biochar derived from glucose by activating it with KOH and incorporating nitrogen at a pyrolysis temperature of 800 °C [126]. This modification endowed the biochar with a substantial Cr (VI) adsorption capability of 402.9 mg/g. The adsorption process involved a combination of mechanisms, including physical adsorption, electrostatic attraction, surface complexation, and the reduction of Cr (VI) to Cr (III), followed by the adsorption and precipitation of the reduced Cr (III) species.

Other mechanisms like physical adsorption and micropore filling can also be involved in heavy metal removal. The porous nature of biochar provides a large surface area that facilitates the physical adsorption of metal ions. This is a non-specific process where metal ions are retained on the surface of biochar through van der Waals forces [122]. In the micropore filling, heavy metal ions may get trapped within the micropores of the biochar, especially if the pore size is compatible with the size of the metal ions.

4.2. Mechanisms involved in organic pollutant removal

Organic pollutants such as dyes, pesticides, antibiotics, plasticizers, PAHs, and phenols represent significant categories of contaminants in the environment. The primary removal mechanisms for these common organic pollutants by nano-modified biochars are depicted in Fig. 4. The adsorption of organic contaminants on biochar is controlled by several mechanisms, predominantly including pore-filling, π–π interactions, hydrophobic effects, electrostatic attraction, and hydrogen bonding as discussed below.

Pore Filling. The process of pore-filling plays a crucial role in the adsorption of organic substances onto biochar. The capacity for adsorption is directly proportional to the surface area of the micropores [127]. Chen et al. discovered that the surface area of biochar, which affects the adsorption rate of naphthalene (NAP) in solutions, is determined by the temperature at which the biochar is pyrolyzed [128]. Higher pyrolysis temperatures lead to more complete carbonization of the organic components in the biomass, resulting in biochar with a greater degree of carbonization, a larger surface area, and more developed micropores, all of which contribute to a higher sorption rate. Zhu et al. also noted that the extensive surface area and pore volume of carbon-based materials typically enhance the sorption of organic pollutants due to the pore-filling effect [129].

π–π Interactions. Many organic pollutants have aromatic components that can undergo π–π electron donor-acceptor interactions with aromatic regions in biochar. Xie et al. reported a strong correlation between the adsorption of sulfonamides (SAs) and the degree of graphitization of various biochars [130]. They attributed this correlation to the π-π electron donor-acceptor (EDA) interactions that occur between the graphitic surfaces of the biochars (which act as π electron donors) and the SAs (which act as π electron acceptors), leading to the pronounced adsorption observed. In a different study, a graphene oxide-modified magnetic sludge biochar (GO/Co-Fe_2O_4-S biochar) was developed for the removal of the pesticide imidacloprid [131]. They observed a maximum adsorption capacity of 8.64 mg/g for imidacloprid on GO/$CoFe_2O_4$-S biochar.This was attributed to the increased surface area, the π-π conjugation interactions between the graphitic structures/−OH groups and the pollutant, and the abundance of available binding sites such as C–O, Fe–O, and Co–O.

Hydrophobic Interactions. The non-polar domains of biochar can sequester non-polar organic compounds, removing them from the aqueous phase. For example, the use of engineered biochar for the elimination of antibiotics has been well-documented. Zeng et al. activated coffee ground-derived biochar with H_3PO_4 to target the adsorption of sulfadiazine [132]. The biochar's modification led to a significant uptake capacity for sulfadiazine, reaching 139.2 mg/g, which was primarily due to the hydrophobic effect and π–π electron donor-acceptor (EDA) interactions.

Additionally, hydrogen bonding, electrostatic forces, and hydrophobic interactions are the prevalent processes for the removal of organic pollutants in the natural environment. For instance, a sulfur-doped biochar derived from tapioca peel waste proved to be an effective adsorbent for malachite green (30.2 mg/g) and rhodamine B (33.1 mg/g), with electrostatic attraction, surface complexation, and hydrogen bonding identified as the primary mechanisms for their removal [133].

5. Future directions

The next phase of research should build upon the solid foundation laid by current studies, pushing the boundaries of innovation towards sustainable and scalable solutions. Below are outlined key areas where focused efforts could yield substantial advancements, further solidifying the role of nano-modified biochar in environmental remediation.

5.1. Advancements in synthesis methods

The synthesis of nano-modified biochar is a critical area where innovation can significantly amplify its utility and efficiency. Future research should prioritize the development of novel synthesis methods that enhance the intrinsic properties of nano-modified biochar, such as increased surface area, porosity, and reactivity. These improvements could dramatically elevate its adsorption capacity and effectiveness in pollutant removal. There is a growing need to refine current methods to make them more energy-efficient and environmentally benign. The exploration of low-temperature synthesis processes, or the utilization of renewable energy sources, could contribute to more sustainable production practices. Another key area is the scalability of synthesis methods. The transition from lab-scale to industrial-scale production often presents challenges in maintaining the quality and characteristics of nano-modified biochar. Research into scalable production techniques that can be consistently reproduced will be crucial for widespread application. The field could also benefit from the exploration of new synthesis techniques, such as microwave-assisted pyrolysis or hydrothermal carbonization, which might offer unique advantages in terms of yield, quality, and environmental impact. Tailoring the properties of nano-modified biochar to target specific pollutants or environmental conditions is another promising direction. This might involve manipulating the feedstock or the synthesis conditions to produce nano-modified biochar with specific characteristics suited to target remediation needs.

5.2. Enhancing environmental sustainability in biochar production

In addressing the environmental concerns associated with the calcination process inherent in biochar production, recent research underscores the importance of implementing innovative strategies to mitigate emissions and optimize sustainability. Optimization of pyrolysis conditions has been demonstrated to significantly reduce the emission of greenhouse gases and volatile organic compounds [134]. The integration of advanced emission control technologies, such as scrubbers and catalytic converters, further enables the effective capture of pollutants, thereby minimizing atmospheric emissions [135]. Selecting appropriate biomass feedstocks,

particularly those that are waste-derived, can also play a crucial role in reducing environmental impacts by diverting waste from landfills and reducing methane emissions [136]. Importantly, life cycle assessments of biochar systems reveal that, when considering the full production and application cycle, biochar can offer a net positive environmental impact, particularly in terms of carbon sequestration and soil health improvement, thereby offsetting the emissions generated during its production [137]. These strategies collectively underscore the multifaceted approach required to address the environmental challenges of biochar production, emphasizing the need for a balanced assessment of both its potential environmental impacts and its substantial benefits in environmental remediation applications.

5.3. Assessing and managing the environmental fate of pollutants in nano-modified biochar applications

It is pivotal to address the bioavailability and environmental fate of pollutants once immobilized by these advanced materials. While nano-modified biochar demonstrates a high capacity for adsorbing and immobilizing various pollutants due to its large surface area and enhanced reactivity, the potential for re-release of these pollutants into the environment is a subject of ongoing research. Factors such as environmental conditions, the properties of the pollutants, and the physical and chemical characteristics of nano-modified biochar play crucial roles in this process. An illustrative example of this is the significant impact that environmental pH levels have on the biogeochemical activities of nano-modified biochar in environmental remediation efforts. Research by Gaya et al. demonstrates that in acidic (low pH) environments, the functional groups on nano-modified biochar are prone to protonation, leading to the formation of H^+ ions [138]. This process initiates a competitive interaction between H^+ ions and cationic pollutants for the cation adsorption sites available on the nano-modified biochar, thereby reducing its pollutant adsorption capacity, as further evidenced in the studies by Mahmoud et al. and Park et al. [139,140]. Additionally, it was reported that at high pH levels, the surface of nano-modified biochar, which carries a negative charge, exhibits a lower affinity for negatively charged or neutral pollutants due to electrostatic repulsion, further complicating the dynamics of pollutant adsorption. Therefore, it becomes crucial to monitor pH variations in the environment when employing nano-modified biochar for the purpose of environmental remediation. Adding to this, when nano-modified biochar is introduced into the environment, its ability to stabilize a significant number of pollutants can considerably decrease their transport and bioavailability, thereby mitigating their impact on ecosystems and human health. Yet, the possibility of immobilized pollutants being released back into the environment remains an unresolved question. This underscores the challenge of retrieving used biochar from the environment for remediation purposes. Given the nano-scale size of nano-modified biochar, recycling it poses an even greater challenge. Consequently, the development of nano-modified biochar recovery technologies and a deeper understanding of its environmental risks for post-pollutant adsorption warrant further investigation. In addition to the factors previously mentioned that influence the environmental fate of pollutants immobilized by nano-modified biochar, the interactions between nano-modified biochar and plant systems represent a critical area for future investigation. Plants can play a significant role in the uptake and transport of biochar nanoparticles, potentially leading to bioaccumulation and trophic transfer in the food chain. Consequently, future studies should assess the extent to which nano-modified biochar is taken up by root systems, its translocation within plant tissues, and its eventual fate in terms of bioaccumulation and potential food chain transfer. Such research is vital to fully understand the ecological risks and to develop strategies to mitigate any negative impacts, ensuring that nano-modified biochar applications in environmental remediation do not inadvertently pose a threat to ecosystem health or food safety.

5.4. Material modification and functionalization

The versatility of nano-modified biochar can be significantly enhanced through strategic material modification and functionalization. This area of research holds the key to unlocking the full potential of nano-modified biochar's in environmental applications, particularly pollutant removal. Tailoring the surface properties of nano-modified biochar through chemical or physical modifications can significantly improve its affinity for specific pollutants. Investigating various functional groups that can be introduced onto the biochar surface could lead to more selective and efficient adsorption processes. The development of nano-modified biochar-based hybrid materials is an exciting prospect. By combining nano-modified biochar with other materials such as metal oxides, graphene, or polymers, the resultant composites could exhibit synergistic properties, enhancing both capacity and selectivity for pollutant removal. Future research should focus on customizing nano-modified biochar for specific pollutants, which could involve modifying it to improve its efficiency in adsorbing and breaking down complex organic compounds or heavy metals. Improving the stability and reusability of nano-modified biochar is crucial for its practical application. Studies that investigate how modifications impact the durability and regeneration capacity of nano-modified biochar can lead to more sustainable and economically viable solutions.

6. Conclusion

In this review, we have comprehensively discussed the modification and functionalization of nano-modified biochars, delving into various preparation and characterization techniques of biochar-MNPs. We also shed light on the use of these nano-modified biochars in remediating natural environments where water and soil are contaminated with both heavy metals and organic substances. The review also reveals that certain characteristics of nano-modified biochars, such as enhanced surface area, addition of functional groups, and improved electron transport capacity, are crucial in boosting their efficiency for multifaceted decontamination purposes. Future studies should delve deeper into the biogeochemical behavior of nano-modified biochar, exploring how its interactions with soil and water matrices affect the long-term stability and efficacy of contaminant immobilization. Additionally, understanding the bioavailability of pollutants in the presence of nano-modified biochar is crucial for evaluating its environmental safety and effectiveness.

Research in these areas will not only broaden our comprehension of nano-modified biochar's environmental interactions but also refine its applications for sustainable remediation. As nano-modified biochar continues to emerge as a versatile tool for environmental challenges, its integration into broader ecological conservation strategies offers a promising path towards achieving a cleaner and more sustainable planet.

Data availability

No data was generated or used for the research described in the review article.

CRediT authorship contribution statement

Neda Arabzadeh Nosratabad: Writing – review & editing, Writing – original draft. **Qiangu Yan:** Writing – review & editing, Conceptualization. **Zhiyong Cai:** Writing – review & editing, Conceptualization. **Caixia Wan:** Writing – review & editing, Project administration, Conceptualization.

Declaration of competing interest

The authors declare that they have no known competing financial interests or personal relationships that could have appeared to influence the work reported in this paper.

Acknowledgements

The authors thank the financial support from the USDA Forest Service (Grant No. 23-JV-11111124-053 and 24-JV-11111124-017).

References

[1] Ramlan, et al., Pollution and contamination level of Cu, Cd, and Hg heavy metals in soil and food crop, Int. J. Environ. Sci. Technol. 19 (2022) 1153–1164, https://doi.org/10.1007/s13762-021-03345-8.
[2] A. Kumar, et al., Lead toxicity: health hazards, influence on food chain, and sustainable remediation approaches, Int. J. Environ. Res. Publ. Health 17 (2020) 2179, https://doi.org/10.3390/ijerph17072179.
[3] V. Antoniadis, et al., A critical prospective analysis of the potential toxicity of trace element regulation limits in soils worldwide: are they protective concerning health risk assessment?-A review, Environ. Int. 127 (2019) 819–847, https://doi.org/10.1016/j.envint.2019.03.039.
[4] S.M. Shaheen, et al., Manganese oxide-modified biochar: production, characterization and applications for the removal of pollutants from aqueous environments-a review, Bioresour. Technol. 346 (2022) 126581, https://doi.org/10.1016/j.biortech.2021.126581.
[5] G. Dönmez, N. Koçberber, Isolation of hexavalent chromium resistant bacteria from industrial saline effluents and their ability of bioaccumulation, Enzym. Microb. Technol. 36 (2005) 700–705, https://doi.org/10.1016/j.enzmictec.2004.12.025.
[6] N.S. Abadeer, et al., Distance and plasmon wavelength dependent fluorescence of molecules bound to silica-coated gold nanorods, ACS Nano 8 (2014) 8392–8406, https://doi.org/10.1021/nn502887j.
[7] W. Liu, et al., Treatment of CrVI-containing Mg (OH) 2 nanowaste, Angew. Chem. 120 (2008) 5701–5704, https://doi.org/10.1002/ange.200800172.
[8] D.S. Kacholi, M. Sahu, Levels and health risk assessment of heavy metals in soil, water, and vegetables of Dar es Salaam, Tanzania, J. Chem. 2018 (2018) 1–9, https://doi.org/10.1155/2018/1402674.
[9] A. Kumar, et al., Biochar as environmental armour and its diverse role towards protecting soil, water and air, Sci. Total Environ. 806 (2022) 150444, https://doi.org/10.1016/j.scitotenv.2021.150444.
[10] J. Schwartz, Short term fluctuations in air pollution and hospital admissions of the elderly for respiratory disease, Thorax 50 (1995) 531–538, https://doi.org/10.1136/thx.50.5.531.
[11] J.H. Seinfeld, S.N. Pandis, Atmospheric Chemistry and Physics: from Air Pollution to Climate Change, John Wiley & Sons, 2016.
[12] S.A. Bhat, et al., Sustainable nanotechnology based wastewater treatment strategies: achievements, challenges and future perspectives, Chemosphere 288 (2022) 132606, https://doi.org/10.1016/j.chemosphere.2021.132606.
[13] Z. Yu, et al., Physiological and biochemical effects of polystyrene micro/nano plastics on Arabidopsis thaliana, J. Hazard Mater. 469 (2024) 133861, https://doi.org/10.1016/j.jhazmat.2024.133861.
[14] J. Lehmann, A handful of carbon, Nature 447 (2007) 143–144, https://doi.org/10.1038/447143a.
[15] Z. Liu, et al., Modified biochar: synthesis and mechanism for removal of environmental heavy metals, Carbon Research 1 (2022) 8, https://doi.org/10.1007/s44246-022-00007-3.
[16] S.O. Amusat, et al., Ball-milling synthesis of biochar and biochar–based nanocomposites and prospects for removal of emerging contaminants: a review, J. Water Process Eng. 41 (2021) 101993, https://doi.org/10.1016/j.jwpe.2021.101993.
[17] D.A. Wardle, M.-C. Nilsson, O. Zackrisson, Fire-derived charcoal causes loss of forest humus, Science 320 (2008), https://doi.org/10.1126/science.1154960, 629-629.
[18] M. Marcińczyk, P. Oleszczuk, Biochar and engineered biochar as slow-and controlled-release fertilizers, J. Clean. Prod. 339 (2022) 130685, https://doi.org/10.1016/j.jclepro.2022.130685.
[19] Y. Zhang, J. Wang, Y. Feng, The effects of biochar addition on soil physicochemical properties: a review, Catena 202 (2021) 105284, https://doi.org/10.1016/j.catena.2021.105284.
[20] Q. Jia, et al., Zea mays cultivation, biochar, and arbuscular mycorrhizal fungal inoculation influenced lead immobilization, Microbiol. Spectr. 12 (2024) e03427, https://doi.org/10.1128/spectrum.03427-23, 23.
[21] S. Elkhalifa, et al., Food waste to biochars through pyrolysis: a review, Resour. Conserv. Recycl. 144 (2019) 310–320, https://doi.org/10.1016/j.resconrec.2019.01.024.
[22] Z. Zhang, et al., Insights into biochar and hydrochar production and applications: a review, Energy 171 (2019) 581–598, https://doi.org/10.1016/j.energy.2019.01.035.
[23] M.B. Ahmed, et al., Progress in the preparation and application of modified biochar for improved contaminant removal from water and wastewater, Bioresour. Technol. 214 (2016) 836–851, https://doi.org/10.1016/j.biortech.2016.05.057.
[24] T. Sizmur, et al., Biochar modification to enhance sorption of inorganics from water, Bioresour. Technol. 246 (2017) 34–47, https://doi.org/10.1016/j.biortech.2017.07.082.

[25] F.R. Oliveira, et al., Environmental application of biochar: current status and perspectives, Bioresour. Technol. 246 (2017) 110–122, https://doi.org/10.1016/j.biortech.2017.08.122.
[26] N.A. Awang, et al., A review on preparation, surface enhancement and adsorption mechanism of biochar-supported nano zero-valent iron adsorbent for hazardous heavy metals, J. Chem. Technol. Biotechnol. 98 (2023) 22–44, https://doi.org/10.1002/jctb.7182.
[27] J.F. Chin, et al., Recent development of magnetic biochar crosslinked chitosan on heavy metal removal from wastewater–modification, application and mechanism, Chemosphere 291 (2022) 133035, https://doi.org/10.1016/j.chemosphere.2021.133035.
[28] V.H. Grassian, When size really matters: size-dependent properties and surface chemistry of metal and metal oxide nanoparticles in gas and liquid phase environments, J. Phys. Chem. C 112 (2008) 18303–18313, https://doi.org/10.1021/jp806073t.
[29] S.R. Emory, W.E. Haskins, S. Nie, Direct observation of size-dependent optical enhancement in single metal nanoparticles, J. Am. Chem. Soc. 120 (1998) 8009–8010, https://doi.org/10.1021/ja9815677.
[30] Y.H. Teow, A.W. Mohammad, New generation nanomaterials for water desalination: a review, Desalination 451 (2019) 2–17, https://doi.org/10.1016/j.desal.2017.11.041.
[31] O.M. Rodriguez-Narvaez, et al., Biochar-supported nanomaterials for environmental applications, J. Ind. Eng. Chem. 78 (2019) 21–33, https://doi.org/10.1016/j.jiec.2019.06.008.
[32] K. Premarathna, et al., Biochar-based engineered composites for sorptive decontamination of water: a review, Chem. Eng. J. 372 (2019) 536–550, https://doi.org/10.1016/j.cej.2019.04.097.
[33] K. Thines, et al., Synthesis of magnetic biochar from agricultural waste biomass to enhancing route for waste water and polymer application: a review, Renew. Sustain. Energy Rev. 67 (2017) 257–276, https://doi.org/10.1016/j.rser.2016.09.057.
[34] H. Sultan, et al., Biochar and nano biochar: enhancing salt resilience in plants and soil while mitigating greenhouse gas emissions: a comprehensive review, Environ. Manag. 355 (2024) 120448, https://doi.org/10.1016/j.jenvman.2024.120448.
[35] R. Li, et al., An overview of carbothermal synthesis of metal–biochar composites for the removal of oxyanion contaminants from aqueous solution, Carbon 129 (2018) 674–687, https://doi.org/10.1016/j.carbon.2017.12.070.
[36] X.-f. Tan, et al., Biochar-based nano-composites for the decontamination of wastewater: a review, Bioresour. Technol. 212 (2016) 318–333, https://doi.org/10.1016/j.biortech.2016.04.093.
[37] R. Ahuja, et al., Nano modifications of biochar to enhance heavy metal adsorption from wastewaters: a review, ACS Omega 7 (2022) 45825–45836, https://doi.org/10.1021/acsomega.2c05117.
[38] O. Mašek, et al., Influence of production conditions on the yield and environmental stability of biochar, Fuel 103 (2013) 151–155, https://doi.org/10.1016/j.fuel.2011.08.044.
[39] A. Demirbas, Effects of temperature and particle size on bio-char yield from pyrolysis of agricultural residues, J. Anal. Appl. Pyrolysis 72 (2004) 243–248, https://doi.org/10.1016/j.jaap.2004.07.003.
[40] M. Jiang, et al., Nanobiochar for the remediation of contaminated soil and water: challenges and opportunities, Biochar 5 (2023) 2, https://doi.org/10.1007/s42773-022-00201-x.
[41] T. Alsawy, et al., A comprehensive review on the chemical regeneration of biochar adsorbent for sustainable wastewater treatment, Npj Clean Water 5 (2022) 29, https://doi.org/10.1038/s41545-022-00172-3.
[42] P. Singh, et al., Sustainable low-concentration arsenite [As (III)] removal in single and multicomponent systems using hybrid iron oxide–biochar nanocomposite adsorbents—a mechanistic study, ACS Omega 5 (2020) 2575–2593, https://doi.org/10.1021/acsomega.9b02842.
[43] M. Zhang, B. Gao, Removal of arsenic, methylene blue, and phosphate by biochar/AlOOH nanocomposite, Chem. Eng. J. (Lausanne) 226 (2013) 286–292, https://doi.org/10.1016/j.cej.2013.04.077.
[44] K.-W. Jung, K.-H. Ahn, Fabrication of porosity-enhanced MgO/biochar for removal of phosphate from aqueous solution: application of a novel combined electrochemical modification method, Bioresour. Technol. 200 (2016) 1029–1032, https://doi.org/10.1016/j.biortech.2015.10.008.
[45] A.Y. Li, et al., Superefficient removal of heavy metals from wastewater by Mg-loaded biochars: adsorption characteristics and removal mechanisms, Langmuir 36 (2020) 9160–9174, https://doi.org/10.1021/acs.langmuir.0c01454.
[46] C. Li, et al., Facile synthesis of nano ZnO/ZnS modified biochar by directly pyrolyzing of zinc contaminated corn stover for Pb (II), Cu (II) and Cr (VI) removals, Waste Manag. 79 (2018) 625–637, https://doi.org/10.1016/j.wasman.2018.08.035.
[47] N. Chaukura, E.C. Murimba, W. Gwenzi, Synthesis, characterisation and methyl orange adsorption capacity of ferric oxide–biochar nano-composites derived from pulp and paper sludge, Appl. Water Sci. 7 (2017) 2175–2186, https://doi.org/10.1007/s13201-016-0392-5.
[48] F. Yang, et al., A novel electrochemical modification combined with one-step pyrolysis for preparation of sustainable thorn-like iron-based biochar composites, Bioresour. Technol. 274 (2019) 379–385, https://doi.org/10.1016/j.biortech.2018.10.042.
[49] N. Zhu, et al., Adsorption of arsenic, phosphorus and chromium by bismuth impregnated biochar: adsorption mechanism and depleted adsorbent utilization, Chemosphere 164 (2016) 32–40, https://doi.org/10.1016/j.chemosphere.2016.08.036.
[50] F. Omidvar-Hosseini, F. Moeinpour, Removal of Pb (II) from aqueous solutions using Acacia Nilotica seed shell ash supported Ni0. 5Zn0. 5Fe2O4 magnetic nanoparticles, J. Water Reuse Desalin. 6 (2016) 562–573, https://doi.org/10.2166/wrd.2016.073.
[51] Q. Chen, et al., Synthesis of a stable magnesium-impregnated biochar and its reduction of phosphorus leaching from soil, Chemosphere 199 (2018) 402–408, https://doi.org/10.1016/j.chemosphere.2018.02.058.
[52] V. Gupta, A. Nayak, Cadmium removal and recovery from aqueous solutions by novel adsorbents prepared from orange peel and Fe2O3 nanoparticles, Chem. Eng. J. (Lausanne) 180 (2012) 81–90, https://doi.org/10.1016/j.cej.2011.11.006.
[53] L. Dai, et al., Calcium-rich biochar from the pyrolysis of crab shell for phosphorus removal, J. Environ. Manag. 198 (2017) 70–74, https://doi.org/10.1016/j.jenvman.2017.04.057.
[54] M. Inyang, et al., Synthesis, characterization, and dye sorption ability of carbon nanotube–biochar nanocomposites, Chem. Eng. J. (Lausanne) 236 (2014) 39–46, https://doi.org/10.1016/j.cej.2013.09.074.
[55] S.A. Jabasingh, H. Belachew, A. Yimam, Iron oxide induced bagasse nanoparticles for the sequestration of Cr6+ ions from tannery effluent using a modified batch reactor, J. Appl. Polym. Sci. 135 (2018) 46683, https://doi.org/10.1002/app.46683.
[56] H. Zhang, et al., Enhanced removal of heavy metal ions from aqueous solution using manganese dioxide-loaded biochar: behavior and mechanism, Sci. Rep. 10 (2020) 6067, https://doi.org/10.1038/s41598-020-63000-z.
[57] L. Zhou, et al., Adsorption properties of nano-MnO2–biochar composites for copper in aqueous solution, Molecules 22 (2017) 173, https://doi.org/10.3390/molecules22010173.
[58] Z.-H. Diao, et al., Insights into the simultaneous removal of Cr6+ and Pb2+ by a novel sewage sludge-derived biochar immobilized nanoscale zero valent iron: coexistence effect and mechanism, Sci. Total Environ. 642 (2018) 505–515, https://doi.org/10.1016/j.scitotenv.2018.06.093.
[59] J. Kim, et al., Application of iron-modified biochar for arsenite removal and toxicity reduction, J. Ind. Eng. Chem. 80 (2019) 17–22, https://doi.org/10.1016/j.jiec.2019.07.026.
[60] S. Wan, et al., Functionalizing biochar with Mg–Al and Mg–Fe layered double hydroxides for removal of phosphate from aqueous solutions, J. Ind. Eng. Chem. 47 (2017) 246–253, https://doi.org/10.1016/j.jiec.2016.11.039.
[61] A. Tomczyk, K. Szewczuk-Karpisz, Effect of biochar modification by vitamin c, hydrogen peroxide or silver nanoparticles on its physicochemistry and tetracycline removal, Materials 15 (2022) 5379, https://doi.org/10.3390/ma15155379.
[62] X. Zhang, R. Sun, Construction of an electrochemical sensor for detection of nitrite by gold nanoparticles immobilized on biochar, Int. J. Electrochem. Sci. (2023) 100219, https://doi.org/10.1016/j.ijoes.2023.100219.
[63] J. Wang, et al., Gold nanoparticles decorated biochar modified electrode for the high-performance simultaneous determination of hydroquinone and catechol, Sensor. Actuator. B Chem. 306 (2020) 127590, https://doi.org/10.1016/j.snb.2019.127590.

[64] S. Zhu, et al., Magnetic nanoscale zerovalent iron assisted biochar: interfacial chemical behaviors and heavy metals remediation performance, ACS Sustain. Chem. Eng. 5 (2017) 9673–9682, https://doi.org/10.1021/acssuschemeng.7b00542.
[65] T. Liao, et al., La (OH) 3-modified magnetic pineapple biochar as novel adsorbents for efficient phosphate removal, Bioresour. Technol. 263 (2018) 207–213, https://doi.org/10.1016/j.biortech.2018.04.108.
[66] H. Arabyarmohammadi, et al., Utilization of a novel chitosan/clay/biochar nanobiocomposite for immobilization of heavy metals in acid soil environment, J. Polym. Environ. 26 (2018) 2107–2119, https://doi.org/10.1007/s10924-017-1102-6.
[67] P. Daraei, et al., Novel thin film composite membrane fabricated by mixed matrix nanoclay/chitosan on PVDF microfiltration support: preparation, characterization and performance in dye removal, J. Membr. Sci. 436 (2013) 97–108, https://doi.org/10.1016/j.memsci.2013.02.031.
[68] B. Krajewska, Diffusion of metal ions through gel chitosan membranes, React. Funct. Polym. 47 (2001) 37–47, https://doi.org/10.1016/S1381-5148(00)00068-7.
[69] G. Liu, et al., Formation and physicochemical characteristics of nano biochar: insight into chemical and colloidal stability, Environ. Sci. Technol. 52 (2018) 10369–10379, https://doi.org/10.1021/acs.est.8b01481.
[70] D. Wang, W. Zhang, D. Zhou, Antagonistic effects of humic acid and iron oxyhydroxide grain-coating on biochar nanoparticle transport in saturated sand, Environ. Sci. Technol. 47 (2013) 5154–5161, https://doi.org/10.1021/es305337r.
[71] M. Kumar, et al., Ball milling as a mechanochemical technology for fabrication of novel biochar nanomaterials, Bioresour. Technol. 312 (2020) 123613, https://doi.org/10.1016/j.biortech.2020.123613.
[72] B. Song, et al., Preparation of nano-biochar from conventional biorefineries for high-value applications, Renew. Sustain. Energy Rev. 157 (2022) 112057, https://doi.org/10.1016/j.rser.2021.112057.
[73] H. Lyu, et al., Effects of ball milling on the physicochemical and sorptive properties of biochar: experimental observations and governing mechanisms, Environ. Pollut. (Amsterdam, Neth.) 233 (2018) 54–63, https://doi.org/10.1016/j.envpol.2017.10.037.
[74] A. Kumar, et al., Sustainable nano-hybrids of magnetic biochar supported g-C3N4/FeVO4 for solar powered degradation of noxious pollutants- Synergism of adsorption, photocatalysis & photo-ozonation, J. Clean. Prod. 165 (2017) 431–451, https://doi.org/10.1016/j.jclepro.2017.07.117.
[75] H. Wu, et al., Modified biochar supported Ag/Fe nanoparticles used for removal of cephalexin in solution: characterization, kinetics and mechanisms, Colloids Surf., A: Physicochem. Eng. 517 (2017) 63–71, https://doi.org/10.1016/j.colsurfa.2017.01.005.
[76] F. Lian, B. Xing, Black carbon (biochar) in water/soil environments: molecular structure, sorption, stability, and potential risk, Environ. Sci. Technol. 51 (2017) 13517–13532, https://doi.org/10.1021/acs.est.7b02528.
[77] Z. Liu, et al., Biochar particle size, shape, and porosity act together to influence soil water properties, PLoS One 12 (2017) e0179079, https://doi.org/10.1371/journal.pone.0179079.
[78] J.J. Pignatello, W.A. Mitch, W. Xu, Activity and reactivity of pyrogenic carbonaceous matter toward organic compounds, Environ. Sci. Technol. 51 (2017) 8893–8908, https://doi.org/10.1021/acs.est.7b01088.
[79] F. Yang, et al., Porous biochar composite assembled with ternary needle-like iron-manganese-sulphur hybrids for high-efficiency lead removal, Bioresour. Technol. 272 (2019) 415–420, https://doi.org/10.1016/j.biortech.2018.10.068.
[80] Y. Xiang, et al., Biochar decorated with gold nanoparticles for electrochemical sensing application, Electrochim. Acta 261 (2018) 464–473, https://doi.org/10.1016/j.electacta.2017.12.162.
[81] C. Wang, H. Wang, Pb(II) sorption from aqueous solution by novel biochar loaded with nano-particles, Chemosphere 192 (2018) 1–4, https://doi.org/10.1016/j.chemosphere.2017.10.125.
[82] B. Yang, et al., Lanthanum ferrite nanoparticles modification onto biochar: derivation from four different methods and high performance for phosphate adsorption, Environ. Sci. Pollut. Res. 26 (2019) 22010–22020, https://doi.org/10.1007/s11356-019-04553-z.
[83] M. Zhang, et al., Synthesis of porous MgO-biochar nanocomposites for removal of phosphate and nitrate from aqueous solutions, Chem. Eng. J. 210 (2012) 26–32, https://doi.org/10.1016/j.cej.2012.08.052.
[84] R. Li, et al., Recovery of phosphate from aqueous solution by magnesium oxide decorated magnetic biochar and its potential as phosphate-based fertilizer substitute, Bioresour. Technol. 215 (2016) 209–214, https://doi.org/10.1016/j.biortech.2016.02.125.
[85] N. Liu, et al., Removal mechanisms of aqueous Cr(VI) using apple wood biochar: a spectroscopic study, J. Hazard Mater. 384 (2020) 121371, https://doi.org/10.1016/j.jhazmat.2019.121371.
[86] Y. Feng, et al., Distribution and speciation of iron in Fe-modified biochars and its application in removal of As(V), As(III), Cr(VI), and Hg(II): an X-ray absorption study, J. Hazard Mater. 384 (2020) 121342, https://doi.org/10.1016/j.jhazmat.2019.121342.
[87] L. Goswami, et al., Nano-biochar as a sustainable catalyst for anaerobic digestion: a synergetic closed-loop approach, Catalysts 12 (2022) 186, https://doi.org/10.3390/catal12020186.
[88] C. Jiang, et al., Converting waste lignin into nano-biochar as a renewable substitute of carbon black for reinforcing styrene-butadiene rubber, Waste Manage. (Tucson, Ariz.) 102 (2020) 732–742, https://doi.org/10.1016/j.wasman.2019.11.019.
[89] C. Xia, et al., Remediation competence of nanoparticles amalgamated biochar (nanobiochar/nanocomposite) on pollutants: a review, Environ. Res. 218 (2023) 114947, https://doi.org/10.1016/j.envres.2022.114947.
[90] J. Yang, et al., Degradation of p-nitrophenol by lignin and cellulose chars: H2O2-mediated reaction and direct reaction with the char, Environ. Sci. Technol. 51 (2017) 8972–8980, https://doi.org/10.1021/acs.est.7b01087.
[91] R. He, et al., Activated biochar with iron-loading and its application in removing Cr (VI) from aqueous solution, Colloids Surf. A Physicochem. Eng. Asp. 579 (2019) 123642, https://doi.org/10.1016/j.colsurfa.2019.123642.
[92] J. Zheng, et al., Levels, spatial distribution, and impact factors of heavy metals in the hair of metropolitan residents in China and human health implications, Environ. Sci. Technol. 55 (2021) 10578–10588, https://doi.org/10.1021/acs.est.1c02001.
[93] X. Wan, C. Li, S.J. Parikh, Simultaneous removal of arsenic, cadmium, and lead from soil by iron-modified magnetic biochar, Environ. Pollut. 261 (2020) 114157, https://doi.org/10.1016/j.envpol.2020.114157.
[94] L. Zhu, et al., Coupling interaction between porous biochar and nano zero valent iron/nano α-hydroxyl iron oxide improves the remediation efficiency of cadmium in aqueous solution, Chemosphere 219 (2019) 493–503, https://doi.org/10.1016/j.chemosphere.2018.12.013.
[95] G. Zhang, et al., Effect of Fe–Mn–Ce modified biochar composite on microbial diversity and properties of arsenic-contaminated paddy soils, Chemosphere 250 (2020) 126249, https://doi.org/10.1016/j.chemosphere.2020.126249.
[96] M.I. Rafique, et al., Immobilization and mitigation of chromium toxicity in aqueous solutions and tannery waste-contaminated soil using biochar and polymer-modified biochar, Chemosphere 266 (2021) 129198, https://doi.org/10.1016/j.chemosphere.2020.129198.
[97] A. Shakya, M. Vithanage, T. Agarwal, Influence of pyrolysis temperature on biochar properties and Cr(VI) adsorption from water with groundnut shell biochars: mechanistic approach, Environ. Res. 215 (2022) 114243, https://doi.org/10.1016/j.envres.2022.114243.
[98] A. Wafiq, D. Reichel, M. Hanafy, Pressure influence on pyrolysis product properties of raw and torrefied Miscanthus: role of particle structure, Fuel 179 (2016) 156–167, https://doi.org/10.1016/j.fuel.2016.03.092.
[99] L. Lian, et al., Globalization-driven industry relocation significantly reduces arctic PAH contamination, Environ. Sci. Technol. 56 (2022) 145–154, https://doi.org/10.1021/acs.est.1c05198.
[100] H. Tian, et al., Degradation prediction and products of polycyclic aromatic hydrocarbons in soils by highly active bimetals/AC-activated persulfate, ACS ES&T Eng. 1 (2021) 1183–1192, https://doi.org/10.1021/acsestengg.1c00063.
[101] H. Li, F. Zhu, S. He, The degradation of decabromodiphenyl ether in the e-waste site by biochar supported nanoscale zero-valent iron/persulfate, Ecotoxicol. Environ. Saf. 183 (2019) 109540, https://doi.org/10.1016/j.ecoenv.2019.109540.
[102] X. Wei, et al., Facile ball-milling synthesis of CuO/biochar nanocomposites for efficient removal of reactive red 120, ACS Omega 5 (2020) 5748–5755, https://doi.org/10.1021/acsomega.9b03787.

[103] S. Ma, et al., New insights into contrasting mechanisms for PAE adsorption on millimeter, micron- and nano-scale biochar, Environ. Sci. Pollut. Res. 26 (2019) 18636–18650, https://doi.org/10.1007/s11356-019-05181-3.
[104] Y. Xu, et al., Effects of Fe-Mn oxide-modified biochar composite applications on phthalate esters (PAEs) accumulation in wheat grains and grain quality under PAEs-polluted brown soil, Ecotoxicol. Environ. Saf. 208 (2021) 111624, https://doi.org/10.1016/j.ecoenv.2020.111624.
[105] M.J. Bentley, et al., Pre-pyrolysis metal and base addition catalyzes pore development and improves organic micropollutant adsorption to pine biochar, Chemosphere 286 (2022) 131949, https://doi.org/10.1016/j.chemosphere.2021.131949.
[106] Y. Zhang, et al., Bacterial response to soil property changes caused by wood ash from wildfire in forest soils around mining areas: relevance of bacterial community composition, carbon and nitrogen cycling, J. Hazard Mater. 412 (2021) 125264, https://doi.org/10.1016/j.jhazmat.2021.125264.
[107] H. Fu, et al., Photochemistry of dissolved black carbon released from biochar: reactive oxygen species generation and phototransformation, Environ. Sci. Technol. 50 (2016) 1218–1226, https://doi.org/10.1021/acs.est.5b04314.
[108] M.M. Ibrahim, et al., Field-applied biochar-based MgO and sepiolite composites possess CO2 capture potential and alter organic C mineralization and C-cycling bacterial structure in fertilized soils, Sci. Total Environ. 813 (2022) 152495, https://doi.org/10.1016/j.scitotenv.2021.152495.
[109] T. Zheng, S. Ouyang, Q. Zhou, Synthesis, characterization, safety design, and application of NPs@ BC for contaminated soil remediation and sustainable agriculture, Biochar 5 (2023) 5, https://doi.org/10.1007/s42773-022-00198-3.
[110] A.E. Creamer, B. Gao, M. Zhang, Carbon dioxide capture using biochar produced from sugarcane bagasse and hickory wood, Chem. Eng. J. 249 (2014) 174–179, https://doi.org/10.1016/j.cej.2014.03.105.
[111] A.E. Creamer, B. Gao, S. Wang, Carbon dioxide capture using various metal oxyhydroxide–biochar composites, Chem. Eng. J. 283 (2016) 826–832, https://doi.org/10.1016/j.cej.2015.08.037.
[112] A. Kumar, et al., Sorption of volatile organic compounds on non-activated biochar, Bioresour. Technol. 297 (2020) 122469, https://doi.org/10.1016/j.biortech.2019.122469.
[113] N. Cheng, et al., Adsorption of emerging contaminants from water and wastewater by modified biochar: a review, Environ. Pollut. 273 (2021) 116448, https://doi.org/10.1016/j.envpol.2021.116448.
[114] T. Ambaye, et al., Mechanisms and adsorption capacities of biochar for the removal of organic and inorganic pollutants from industrial wastewater, Int. J. Environ. Sci. Technol. (2021) 1–22, https://doi.org/10.1007/s13762-020-03060-w.
[115] H. Zhang, et al., Enhanced aqueous Cr (VI) removal using chitosan-modified magnetic biochars derived from bamboo residues, Chemosphere 261 (2020) 127694, https://doi.org/10.1016/j.chemosphere.2020.127694.
[116] H. Chen, et al., KOH modification effectively enhances the Cd and Pb adsorption performance of N-enriched biochar derived from waste chicken feathers, Waste Manag. 130 (2021) 82–92, https://doi.org/10.1016/j.wasman.2021.05.015.
[117] M. Chen, et al., Facilitated transport of cadmium by biochar-Fe3O4 nanocomposites in water-saturated natural soils, Sci. Total Environ. 684 (2019) 265–275, https://doi.org/10.1016/j.scitotenv.2019.05.326.
[118] S. Zhang, et al., A novel biochar supported CMC stabilized nano zero-valent iron composite for hexavalent chromium removal from water, Chemosphere 217 (2019) 686–694, https://doi.org/10.1016/j.chemosphere.2018.11.040.
[119] X. Jia, et al., The antimony sorption and transport mechanisms in removal experiment by Mn-coated biochar, Sci. Total Environ. 724 (2020) 138158, https://doi.org/10.1016/j.scitotenv.2020.138158.
[120] H. Chen, et al., Enhanced sorption of trivalent antimony by chitosan-loaded biochar in aqueous solutions: characterization, performance and mechanisms, J. Hazard Mater. 425 (2022) 127971, https://doi.org/10.1016/j.jhazmat.2021.127971.
[121] L. Wang, et al., Enhanced antimonate (Sb (V)) removal from aqueous solution by La-doped magnetic biochars, Chem. Eng. J. 354 (2018) 623–632, https://doi.org/10.1016/j.cej.2018.08.074.
[122] G. Murtaza, et al., Biochar as a green sorbent for remediation of polluted soils and associated toxicity risks: a critical review, Separations 10 (2023) 197, https://doi.org/10.3390/separations10030197.
[123] C. Yu, et al., Removal of Cu (ii) from aqueous solution using Fe 3 O 4–alginate modified biochar microspheres, RSC Adv. 7 (2017) 53135–53144, https://doi.org/10.1039/C7RA10185F.
[124] Y. Yuan, et al., Applications of biochar in redox-mediated reactions, Bioresour. Technol. 246 (2017) 271–281, https://doi.org/10.1016/j.biortech.2017.06.154.
[125] E. Wen, et al., Iron-modified biochar and water management regime-induced changes in plant growth, enzyme activities, and phytoavailability of arsenic, cadmium and lead in a paddy soil, J. Hazard Mater. 407 (2021) 124344, https://doi.org/10.1016/j.jhazmat.2020.124344.
[126] H. Liang, et al., Preparation of nitrogen-doped porous carbon material by a hydrothermal-activation two-step method and its high-efficiency adsorption of Cr (VI), J. Hazard Mater. 387 (2020) 121987, https://doi.org/10.1016/j.jhazmat.2019.121987.
[127] X. Wang, et al., Recent advances in biochar application for water and wastewater treatment: a review, PeerJ 8 (2020) e9164, https://doi.org/10.7717/peerj.9164.
[128] Z. Chen, B. Chen, C.T. Chiou, Fast and slow rates of naphthalene sorption to biochars produced at different temperatures, Environ. Sci. Technol. 46 (2012) 11104–11111, https://doi.org/10.1021/es302345e.
[129] X. Zhu, et al., A novel porous carbon derived from hydrothermal carbon for efficient adsorption of tetracycline, Carbon 77 (2014) 627–636, https://doi.org/10.1016/j.carbon.2014.05.067.
[130] M. Xie, et al., Adsorption of sulfonamides to demineralized pine wood biochars prepared under different thermochemical conditions, Environ. Pollut. 186 (2014) 187–194, https://doi.org/10.1016/j.envpol.2013.11.022.
[131] Y. Ma, et al., A novel, efficient and sustainable magnetic sludge biochar modified by graphene oxide for environmental concentration imidacloprid removal, J. Hazard Mater. 407 (2021) 124777, https://doi.org/10.1016/j.jhazmat.2020.124777.
[132] X.-Y. Zeng, et al., Impacts of temperatures and phosphoric-acid modification to the physicochemical properties of biochar for excellent sulfadiazine adsorption, Biochar 4 (2022) 14, https://doi.org/10.1007/s42773-022-00143-4.
[133] S. Vigneshwaran, et al., Fabrication of sulfur-doped biochar derived from tapioca peel waste with superior adsorption performance for the removal of Malachite green and Rhodamine B dyes, Surface. Interfac. 23 (2021) 100920, https://doi.org/10.1016/j.surfin.2020.100920.
[134] S. Safarian, Performance analysis of sustainable technologies for biochar production: a comprehensive review, Energy Rep. 9 (2023) 4574–4593, https://doi.org/10.1016/j.egyr.2023.03.111.
[135] S. Li, Reviewing air pollutants generated during the pyrolysis of solid waste for biofuel and biochar production: toward cleaner production practices, Sustainability 16 (2024) 1169, https://doi.org/10.3390/su16031169.
[136] D. Feng, et al., Review of carbon fixation evaluation and emission reduction effectiveness for biochar in China, Energy Fuels 34 (2020) 10583–10606, https://doi.org/10.1021/acs.energyfuels.0c02396.
[137] K.G. Roberts, et al., Life cycle assessment of biochar systems: estimating the energetic, economic, and climate change potential, Environ. Sci. Technol. 44 (2010) 827–833, https://doi.org/10.1021/es902266r.
[138] U.I. Gaya, E. Otene, A.H. Abdullah, Adsorption of aqueous Cd (II) and Pb (II) on activated carbon nanopores prepared by chemical activation of doum palm shell, SpringerPlus 4 (2015) 1–18, https://doi.org/10.1186/s40064-015-1256-4.
[139] M.E. Mahmoud, N.A. Fekry, A.M. Abdelfattah, A novel nanobiosorbent of functionalized graphene quantum dots from rice husk with barium hydroxide for microwave enhanced removal of lead (II) and lanthanum (III), Bioresour. Technol. 298 (2020) 122514, https://doi.org/10.1016/j.biortech.2019.122514.
[140] J.-H. Park, et al., Removing mercury from aqueous solution using sulfurized biochar and associated mechanisms, Environ. Pollut. 244 (2019) 627–635, https://doi.org/10.1016/j.envpol.2018.10.069.